

Battery Module Assembly

Group 61: avk39, mm3491, ss4689, er909

University of Bath

Department of Mechanical Engineering

Design, Materials and Manufacturing 2: ME22007

Word Count: 10272

3.1 PDS

The first stage of designing the machine was creating a product design specification to better understand the functions that would be required of the machine. The PDS (shown below) categorised all these functions into different categories.

Table 1: A product design specification detailing the different demanded and desired functions of the machine

Group 61	Requirements List		Issue 1	
	PRODUCT DESIGN SPECIFICATION		Issue Date	Edited by
D / W	Requirements	Notes		
	1. Performance			
W	The machine will last at least 10 years	Specified by Anna during Q&A session	er909	25/02/2025
D	Over 10 years, the machine will assemble at least 4,861,143 modules	200s cycle, 24 hours/day, 25 weeks/6 months, 10 years, 20% compound efficiency/year	er909	25/02/2025
D	The machine will have the capacity to compound its efficiency by 20% each year	assumed annual increase in demand for battery modules of 20% - from design brief	er909	21/02/2025
W	The machine will operate on a maximum power rating of 15 kW	Very high estimate [1]	er909	21/02/2025
D	The machine will apply a force of 10 N per battery	From design brief	er909	03/03/2025
D	The machine will be able to identify cell polarity	Required to arrange batteries into alternating polarities in the module	er909	24/02/2025
D	Eject modules into conveyor of width 500mm	From design brief	er909	25/02/2025
D	The batteries will be constrained in the vertical direction by a geometric tolerance of 0.5 degrees	From Design Brief	er909	21/02/2025
D	The machine will assemble 65 batteries in a 5 x 13 matrix	From Design Brief	er909	25/02/2025
D	An H7/k6 tolerance fit will be applied to the carrier holes	From Design Brief	er909	25/02/2025
W	The machine will handle multiple modules in parallel to optimise workflow efficiency	Optimise efficiency and reduce cycle time	er909	25/02/2025
D	A maximum of 6 bars will be used for pneumatic systems	From design brief	er909	03/03/2025
D	Top and bottom carriers snap lock together	From design brief	er909	25/02/2025
W	The machine will have important vibration damping to avoid battery misalignment	Due to tight tolerancing and machine vibrations	er909	24/02/2025
D	The machine will have access to a mains source (230V or 415V for three phase supply)	From Design Brief	er909	21/02/2025
D	The assembly of a module will take less than 200s	From design brief	er909	21/02/2025
	2. Physical Characteristics			
D	The machine will take up no more than 15 m^2 of floor area	From design brief (buffers included)	er909	21/02/2025

Battery Module Assembly

W	The machine will not feature a robot arm	From design brief	er909	21/02/2025
D	The machine will fit inside a 30 x 60m plant	From design brief	er909	21/02/2025
W	The machine height will be limited to 5m	Due to temperature variations [2]	er909	21/02/2025
	3. Economic factors			
D	One machine will be produced	From Q&A	er909	25/02/2025
D	Total machine cost must be less than £20,000	From design brief	er909	21/02/2025
	4. Environmental Factors			
W	The machine will operate between 5 and 35 degrees celsius	Due to height and temperature variations [2]	er909	03/03/2025
D	The machine will withstand atmospheric pressure	-	er909	21/02/2025
W	The machine shall be corrosion resistant	Chemical leakages can be highly corrosive [3]	er909	21/02/2025
	5. Legal Factors			
D	The machine will adhere to the british standards for fire safety	Follow Uk gov guidelines for fire safety [4]	er909	21/02/2025
D	The machine will adhere to the british standards for health and safety executive	Follow UK gov guidelines for health and safety executive [5]	er909	25/02/2025
W	The machine will produce minimal waste materials	Key strategies for minimising waste in industries [6]	er909	21/02/2025
W	The machine shall have an enclosed design to prevent exposure to electrical hazards	Protect technicians from electrical hazards and the machine from chemical leakages	er909	24/02/2025
W	The machine will be equipped with an emergency stop button	Equipped for emergency situations	er909	24/02/2025
W	Leakages, electrolyte vapour and venting shall be dedected by safety measures	Following Uk guidelines as well	er909	21/02/2025
W	The plant will be ventilated	Regulate temperature, employee comfort, regulate moisture, dust and air quality management	er909	21/02/2025
W	The machine will be easy to operate	Satisfy technicians as well as chief engineers - machine needs to be useful for everyone	er909	25/02/2025
	6. Quality Assurance			
D	Machine components will be easily accessible for quality control and inspection	Adhere to ISO 9001 for Quality Management Systems [7]	er909	21/02/2025
W	One module in every 3,024 will be assessed for quality control	1 module/week	er909	21/02/2025
	7. Other Considerations			
D	The machine will receive maintenance every 6 months for the duration of one week	From design brief	er909	21/02/2025
W	The machine will produce recyclable modules	PEEK is fully recyclable [8]	er909	24/02/2025

W	Material Handling will be minimised	Providing the right material in the right place at the right time, with the right amount, in the right sequence, and with the right conditions to minimise production cost.	er909	28/02/2025
W	The machine will be made from off the shelf components ideally	From design brief	er909	24/02/2025
W	An instruction manual will be provided with the machine	Ease of use for technicians	er909	21/02/2025
W	A two year guarantee will cover unexpected breakdowns of the machine	Machine should last 10 years, anything <2years is not acceptable	er909	21/02/2025

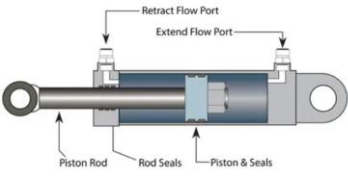
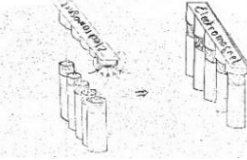
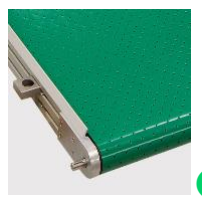
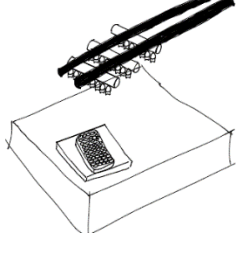
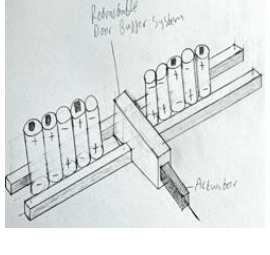
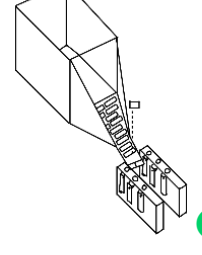
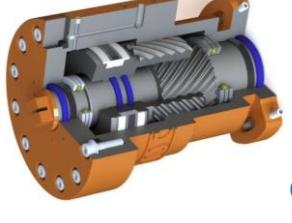
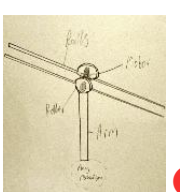
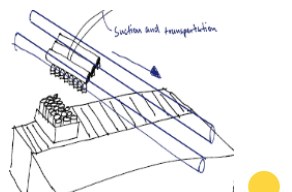
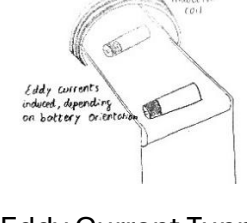
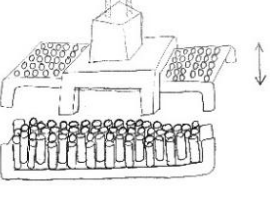
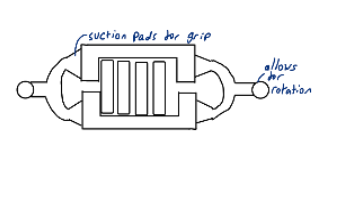
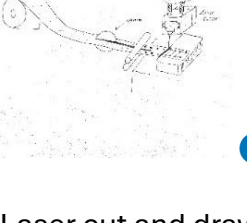
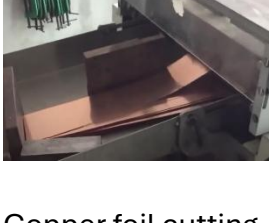
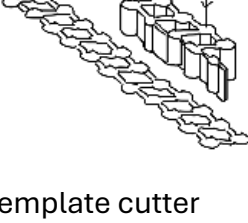
Table 1 details the criteria that make up the product design specification.

References:

- [1] S. Grimsby, "Watts Used By Industrial Machines," *Sciencing*, Sep. 26, 2017. <https://www.scientific.com/watts-used-by-industrial-machines-13662856> (accessed Mar. 14, 2025).
- [2] S. Doroudiani, "Variations of temperatures inside of manufacturing unit at various heights of 1e6 and 6.8m," *Researchgate*, Sep. 2013. https://www.researchgate.net/figure/variations-of-temperatures-inside-of-manufacturing-unit-at-various-heights-of-1e6-and-68_fig7_257171988 (accessed Feb. 21, 2025).
- [3] "Why Batteries Leak | How to Prevent and Clean Corroded Batteries," *Uniross*, Aug. 12, 2024. <https://www.uniross.com/blog/education-2/why-batteries-leak-causes-prevention-tips-and-cleaning-methods-1> (accessed Mar. 14, 2025).
- [4] U. Government, *Fire safety risk assessment*. 2006.
- [5] "Warehousing," *Hse.gov.uk*, 2009. <https://www.hse.gov.uk/logistics/warehousing.htm>
- [6] "Key Strategies for Minimising Waste in Manufacturing Processes," *Institute of Supply Chain Management*, Nov. 15, 2024. <https://www.ioscm.com/blog/key-strategies-for-minimising-waste-in-manufacturing-processes/>
- [7] "Become ISO 9001 certified," *Centre for Assessment*, 2015. <https://www.centreforassessment.co.uk/iso-9001-certification/?msclkid=93b3602b267d132b0793079699d9a3b6> (accessed Mar. 14, 2025).
- [8] "Polyether Ether Ketone (PEEK) Recycling," *AZoM.com*, Dec. 17, 2012. <https://www.azom.com/article.aspx?ArticleID=7989>

3.2 Morphological Chart

After having decided the required functions of the machine (Table 1 above), a morphological chart was then created to provide a clearer and more concise pathway for the initial concepts of the machine. To create the morphological chart, the machine was broken up into its 10 core functions. The team came up with different ways that the machine could execute these functions. This allowed for a more structured concept design phase. The morphological chart can be seen below in Figure 2.

FUNCTION	CONCEPTS
Linear Actuator	   
	Hydraulic Pneumatic Rack and Pinion Scotch Yoke
Cylinder holding	   
	Electromagnet Vacuum Suction Robotic clamp Vacuum Conveyor Belt
Buffer Storage	   
	Spiral Feeder Rail Buffer Door Buffer System Buffer with Separator
Angular Rotation	   
	Rotary Hydraulic System Rotary Electric motor Pneumatic Rotary actuator Wind-Up Spring Mechanism
Support	   
	Rotary Turntable Motor Rail Roller Conveyer Belt XY Manual Slider
Identify Polarity	  
	Eddy Current Tunnel High-Speed Camera No System Used
Clamping	   
	Manual Clamp Over the Head Clamping Top Carrier Clamp Side Clamp
Copper strip division	   
	Laser cut and drawn Copper foil cutting Template cutter Technician

Battery Module Assembly

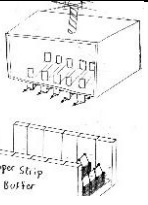
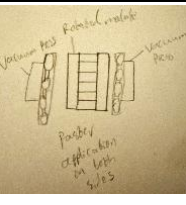
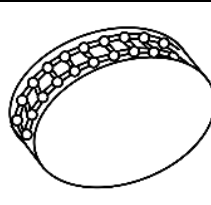
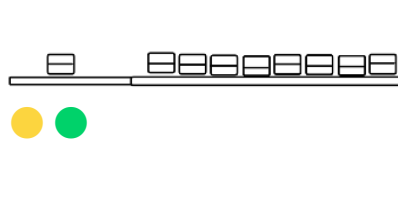
Apply Copper Strips	 Copper Strip Buffer			
	Claw clips	Vacuum Suction	Double Sided Vacuum Suction	Embossed Roller
Ejection				
	Spring Loaded Stacking	Conveyor Buffer	Robot arm Pick and Drop	

Table 2: A morphological chart to shows the ideas sketched in each concept design

 – Concept 1	 – Concept 2
 – Concept 3	 – Concept 4

3.3 Initial Concept Sketches

The next stage of the process involved each team member developing an initial concept design. These designs incorporated various ideas from the morphological chart, as shown in Table 2 above. This approach provided diverse perspectives, which proved invaluable when selecting the final concept later.

From Table 2, Concept 1 uses:

- Rack and pinion actuators
- Robotic clamp
- Spiral feeder buffer
- Hydraulic rotary actuator
- Rotary turntable
- Eddy current tunnel (to identify battery polarity)
- Top carrier clamp
- Drawn and laser cut copper strips
- Claw clips
- Spring loaded stacker

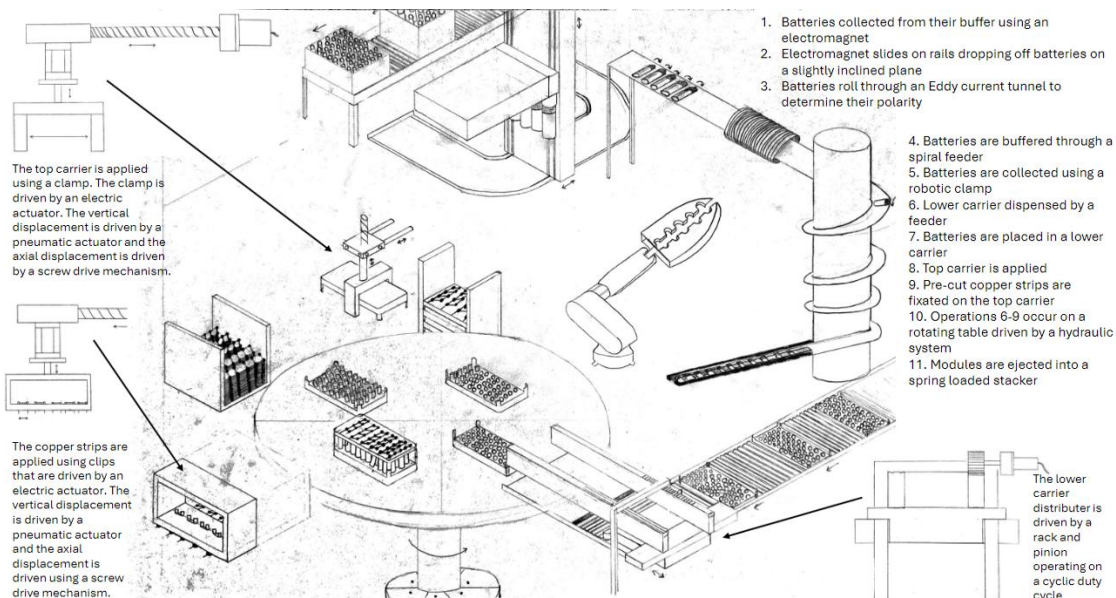


Figure 1: Machine design concept 1

In this concept, batteries are extracted using a rail-mounted electromagnet that moves vertically and horizontally. The support swivels to transfer them onto a gravity-powered conveyor. Misalignment could cause the batteries to drop.

Another issue could arise from the eddy current tunnel to identify battery polarity. The design relies on batteries passing through the tunnel one at a time instead of 5 at a time.

A spiral feeder maintains a steady buffer, optimizing floor space by increasing height instead of width or length. However, once they reach the end of the buffer, concept 1 uses a robotic arm to place five batteries at a time, which was deemed unsuitable per the design brief.

Battery Module Assembly

Lower carriers are distributed via a rack-and-pinion motor, pushing them onto a hydraulically powered rotary turntable. This turntable rotates sequentially, ensuring all four operations occur before advancing. After battery placement, the top carrier is applied using a screwdriver mechanism and an electric actuator with two degrees of freedom.

Copper strips are assumed to be drawn, laser-cut, and buffered before being clipped onto the module. However, their stickiness makes buffering impractical. Additionally, the design fails to meet the brief's final requirement: ejecting modules onto a 500mm-wide conveyer.

From Table 2, Concept 2 uses:

- Hydraulic actuators
- Vacuum conveyor belt
- Polarity separating battery buffer
- Pneumatic rotary actuator
- Roller conveyor belt
- High speed camera
- Side clamp
- Template cutter
- Embossed roller
- Conveyor buffer

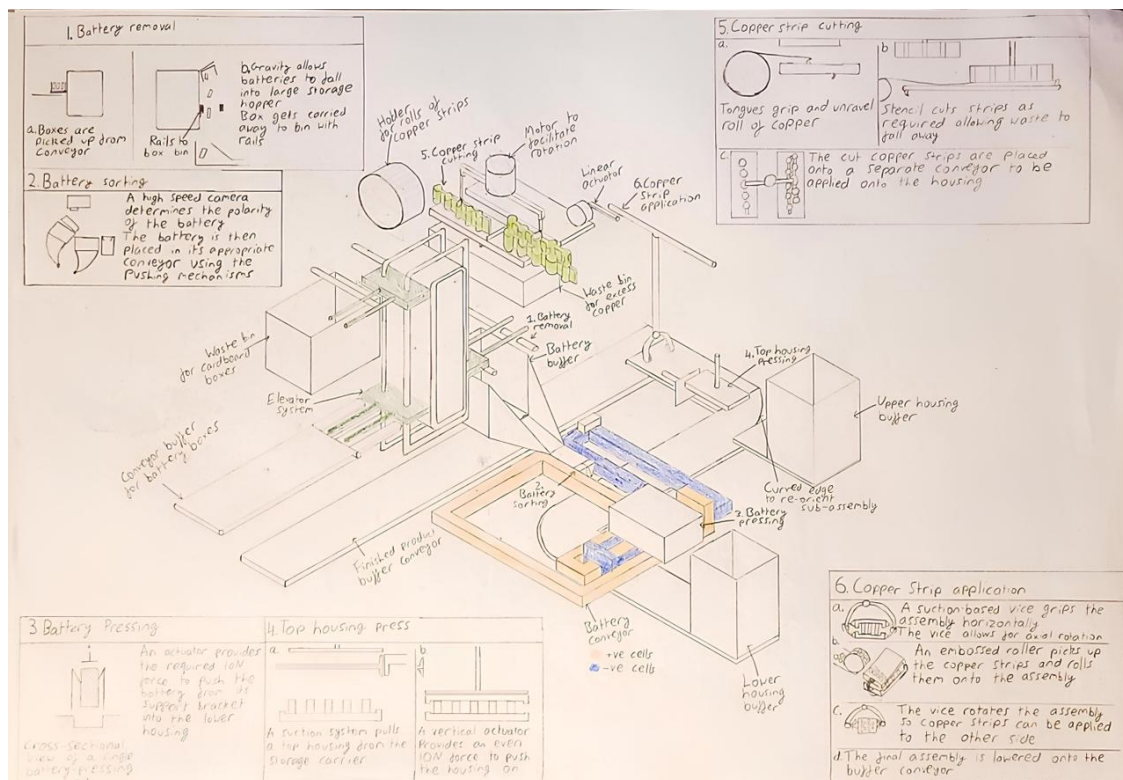


Figure 2: Machine design concept 2

In this concept, battery boxes are picked up from an incoming conveyor via a rail system that rotates 180°, releasing batteries into a large hopper. A key issue is battery misalignment or damage from falling outside the hopper.

Battery Module Assembly

Batteries are then sorted using a high-speed camera that detects polarity and signals a motor to rotate $\pm 90^\circ$, ensuring correct orientation. Once sorted, five batteries drop into a carrier, receiving 10N of force for secure placement. Misalignment could prevent the required $\pm 0.5^\circ$ tolerance, risking battery damage.

Top carriers are retrieved via a suction system, then pressed down by a vertical actuator applying 650N to secure them.

The next step assumes copper rolls are rectangular strips. Tongues clamp the roll's lip, unravelling 13.3 cm before a stencil punches out the required shape. These preforms are buffered onto a separate conveyor, picked up by an embossed roller, and applied to the module. A clamp then rotates the module 180° to apply copper strips to the opposite side. However, deforming the strips around the roller risks damaging the final product.

Finally, the module is lowered onto an exit conveyor.

From Table 2, Concept 3 uses:

- Pneumatic actuator
- Vacuum suction
- Rail buffer
- Rotary electric motor
- XY manual slider
- Overhead clamping
- Copper foil cutting
- Conveyor buffer

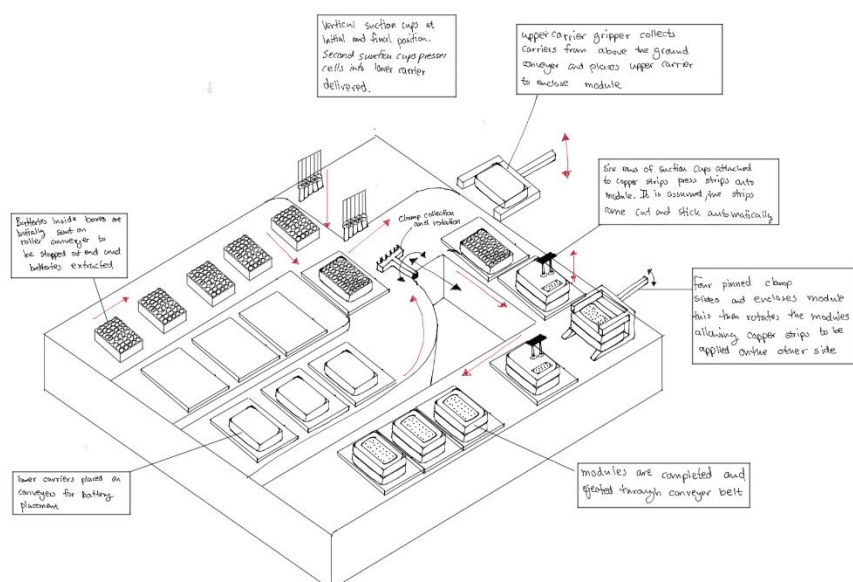


Figure 3: Machine design concept 3

Battery Module Assembly

The design in Figure 3 shows the battery extraction process using suction cups to remove batteries from their boxes and feed them into vertical clamps. These clamps rotate 180° every other cycle to alternate polarity before transferring the batteries to a second set of suction cups, which insert them into lower carriers on a conveyor. A potential issue is interference, as three components operate along the same axis.

Assembled lower carriers move down the line, where an overhead clamp retrieves and secures the top carrier with 650N of force.

Further along, vacuum cups apply buffered copper strips to the module. A clamp then lifts and rotates the module 180° to attach strips to the opposite side. However, this design does not account for dividing the copper strips.

Finally, completed modules are fed onto an exit conveyor.

From Table 2, Concept 4 uses:

- Scotch yoke
- Vacuum suction
- Door buffer system
- Rotary electric motor
- Motor rail
- Overhead clamping
- Assumes the copper strips are precut by technicians
- Double sided vacuum suction
- Robot arm pick and drop

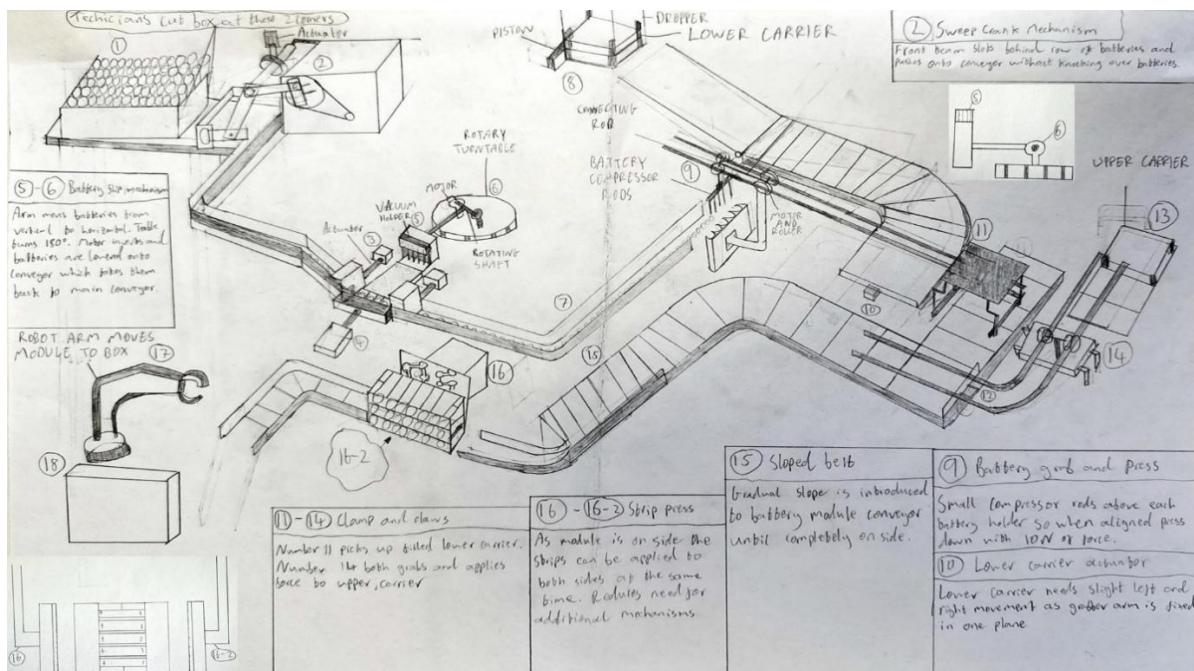


Figure 4: Machine design concept 4

Concept 4 assumes battery boxes arrive with one side cut open. A scotch yoke arm pushes rows of five batteries inward, but this mechanism lacks the two degrees of freedom required for proper movement.

Battery Module Assembly

A door buffer system then separates batteries into sets of five, which are transferred to vacuum cup holders attached to a rotating turntable. As the table rotates 180°, the vacuum arm also rotates 180°, flipping battery orientation every other cycle for correct polarity. However, this process creates a bottleneck, slowing the assembly time.

Lower carriers slide down a conveyor into a station that shifts left and right for battery placement. Suction cups pick up batteries from the buffer, align with the lower carrier using a motorised rail, and release them before compressor rods apply 10N to secure them. Precise timing between suction cup release and rod activation could lead to misalignment.

An overhead clamp transfers the filled lower carrier to a separate conveyor, where another clamp secures it with 650N of force.

The conveyor then tilts 90° to position the module on its side for copper strip application. However, the design does not address how copper strips are divided or applied. Additionally, rotating the conveyor risks the module falling out.

Finally, the module is extracted using a robotic arm, however, this method was deemed unsuitable per the design brief.

3.4 Concept Selection and Evolution & Final Machine Concept Sketch

Each of the four concept sketches will be evaluated using the requirement list from Table 1, ranking them to ensure an informed design selection. The MCDA method was used to rank concepts 1 to 4, using a scoring system that ranged from 1 to 5. Before ranking the concepts by use of the MCDA method, criteria weightings must be defined. This was achieved using the pair wise comparison as can be seen in Table 3. The pair wise comparison ranked each criterion against others and was subsequently attributed a weight from 1 to 10. The highlighted criteria on Table 3, show those that were used to further evaluate the initial concepts.

Criteria	a	b	c	d	e	f	g	h	i	j	k	l	n	n	o	p	q	r	s	t	u	v	w	x	y	z	a	a	a	a	a	a	a	a	a	a	a	a	a	a	a	a	a	a	a	a	a	Total	Rank	Weight (/10)
The machine will last at least 10 years	a	1	1	1	0	1	1	0	0	1	1	1	0	0	0	0	0	1	0	1	1	1	0	0	0	1	0	0	0	1	1	1	1	1	1	21	17	6												
Over 10 years, the machine will assemble at least 4,861,143 modules	b	0	1	1	0	1	1	0	0	1	1	1	0	0	0	1	1	1	0	1	1	1	1	0	0	0	1	0	0	0	1	1	1	1	1	22	16	7												
The machine will have the capacity to compound its efficiency by 20% each year	c	0	0	1	0	1	1	0	0	1	1	1	0	0	0	0	1	1	0	1	1	0	0	0	0	1	1	0	0	1	1	1	1	1	1	19	22	5												
The machine will operate on a maximum power rating of 15 kW	d	0	0	0	0	0	0	1	0	0	0	0	0	0	0	0	0	1	1	0	0	0	0	0	0	0	0	0	0	0	0	0	0	0	0	6	35	2												
The machine will apply a force of 10N to the batteries	e	1	1	1	1	1	1	1	1	1	1	1	0	1	1	1	1	0	1	1	1	1	1	0	1	0	0	1	1	1	1	1	1	1	1	31	10	8												
The machine will be able to identify cell polarity	f	0	0	0	1	0	0	0	0	0	0	1	0	0	0	0	0	1	0	0	0	0	0	0	0	0	0	0	0	0	0	0	0	0	0	4	38	1												
Eject modules into conveyor of width 500mm	g	0	0	0	1	0	1	0	0	0	1	0	0	0	0	1	0	0	0	1	0	0	0	1	1	1	1	1	1	1	1	1	1	1	1	17	24	4												
The batteries will be constrained in the vertical direction by a geometric tolerance of 0.5	h	1	1	1	0	0	1	1	1	0	0	1	1	0	1	0	1	0	1	1	1	1	0	0	0	1	0	0	1	1	1	1	1	1	1	25	15	7												
The machine will assemble 65 batteries in a 5 x 13 matrix	i	1	1	1	0	1	1	1	1	1	1	1	0	1	1	1	1	1	0	1	1	1	1	0	0	0	1	1	1	1	1	1	1	1	1	30	11	8												
An H7/k6 tolerance fit will be applied to the carrier holes	j	0	0	0	1	0	1	1	1	0	1	1	0	0	0	0	1	0	0	1	0	0	0	1	0	0	1	1	1	1	1	1	1	1	1	20	21	5												
The machine will handle multiple modules in parallel to optimise workflow efficiency	k	0	0	0	1	0	1	1	0	0	0	1	0	0	0	0	0	0	1	0	0	0	0	0	0	1	1	0	1	0	1	1	1	1	1	14	27	4												
A maximum of 6 Bar will be used across the machine	l	0	0	0	1	0	0	0	0	0	0	0	0	0	0	0	0	1	0	0	0	0	0	0	0	0	0	0	0	0	0	0	0	0	0	6	35	2												
Top and bottom carriers snap lock together	m	1	1	1	1	1	1	1	1	1	1	1	1	1	1	1	1	1	1	1	1	1	1	1	1	1	1	1	1	1	1	1	1	1	1	30	11	8												
The machine will have important vibration damping to avoid battery misalignment	n	1	1	1	1	0	1	1	0	0	1	1	1	0	1	1	1	1	1	0	0	0	1	0	0	1	1	1	1	1	1	1	1	1	1	26	13	7												
The machine will have access to a mains source (230V or 415V for three phase supply)	o	1	1	1	1	1	1	1	1	1	1	1	1	1	1	1	1	1	1	1	1	1	1	1	1	1	1	1	1	1	1	1	1	1	1	32	8	9												
The assembly of a module will take less than 200s	p	1	0	1	1	0	1	1	0	0	1	1	0	1	0	1	1	1	1	1	1	1	0	0	0	1	1	1	1	1	1	1	1	1	1	26	13	7												
The machine will take up no more than 15 m^2 of floor area	q	1	0	0	0	0	1	1	0	1	1	1	0	0	0	0	0	0	0	1	0	1	1	1	0	0	0	1	1	1	1	1	1	1	1	21	17	6												
The machine will not feature a robot arm	r	0	0	0	0	0	0	0	0	0	1	1	0	0	0	0	1	0	1	0	0	0	0	1	0	0	0	1	0	1	1	1	1	1	1	13	30	3												
The machine will fit inside a 30 x 60m plant	s	1	1	1	1	1	1	1	1	1	1	1	1	1	1	1	1	1	1	1	1	1	1	0	1	0	1	0	0	1	1	1	1	1	1	34	6	9												
The machine height will be limited to 5m	t	0	0	0	1	0	1	0	0	0	0	0	0	0	0	0	0	0	0	0	0	0	0	0	0	0	0	0	0	0	0	0	0	0	0	4	38	1												
One machine will be produced	u	0	0	0	1	0	1	1	0	0	1	1	1	0	0	0	0	1	0	1	0	0	0	0	0	1	0	1	0	1	1	1	1	1	1	18	23	5												
Total machine cost must be less than £20,000	v	0	0	1	1	0	1	1	0	0	1	1	1	0	0	0	0	1	1	1	0	0	0	0	1	0	0	0	1	1	1	1	1	1	1	21	17	6												
The machine will operate between 5 and 35 degrees celsius	w	0	0	0	1	0	1	0	0	0	0	1	0	0	0	0	1	0	1	1	0	0	0	0	0	1	0	0	0	0	1	1	1	1	1	11	31	3												
The machine will withstand atmospheric pressure	x	1	1	1	1	1	1	1	1	1	1	1	1	1	1	1	1	1	1	1	1	1	1	1	1	1	1	1	1	1	1	1	1	1	1	40	1	10												
The machine shall be corrosion resistant	y	1	1	1	1	0	1	1	1	1	1	1	1	1	1	1	1	1	1	1	1	1	0	0	1	0	0	1	1	1	1	1	1	1	1	32	8	9												
The machine will adhere to the british standards for fire safety	z	1	1	1	1	1	1	1	1	1	1	1	1	1	1	1	1	1	1	1	1	1	1	1	1	1	1	1	1	1	1	1	1	1	1	38	2	10												
The machine will adhere to the british standards for health and safety executive	a	1	1	1	1	1	1	1	1	1	1	1	1	1	1	1	1	1	1	1	1	1	1	1	1	1	1	1	1	1	1	1	1	1	1	37	3	10												
The machine will produce minimal waste materials	a	0	0	0	1	0	1	0	0	0	1	1	0	0	0	0	1	0	1	0	1	0	0	0	1	0	1	0	1																					

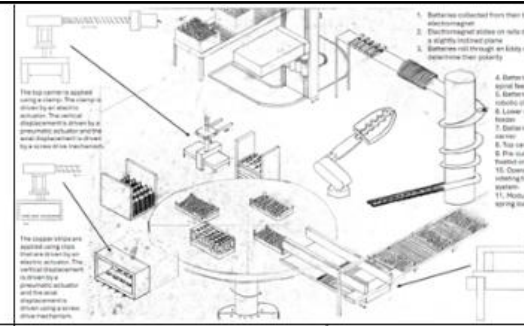
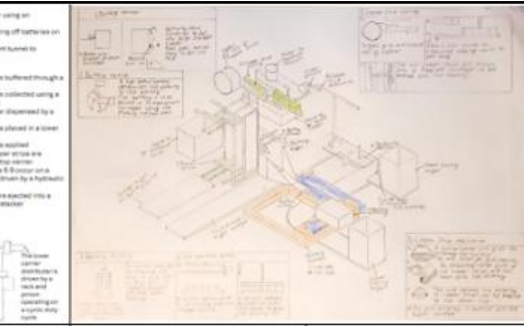
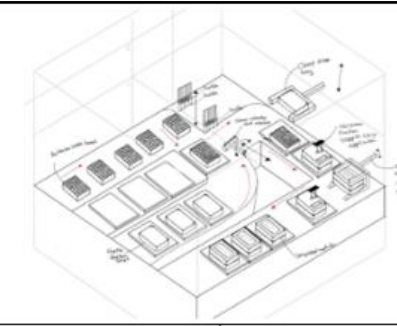
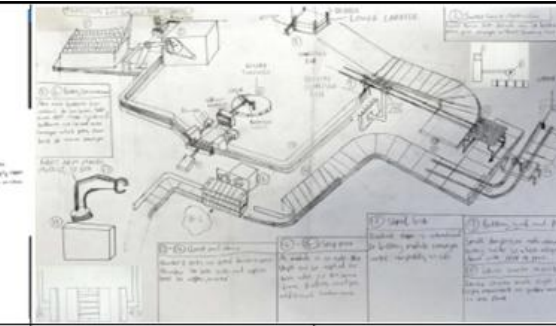
MCDA		Concepts 1-4								
Criteria	Weighting		Score	Weighted score	Score	Weighted Score	Score	Weighted Score	Score	Weighted Score
The machine will have the capacity to compound its efficiency by 20% each year	5		2	10	2	10	4	20	3	15
The machine will be able to identify cell polarity	1		2	2	4	4	1	1	1	1
Eject modules into conveyor of width 500mm	4		0	0	3	12	2	8	3	12
The machine will handle multiple modules in parallel to optimise workflow efficiency	4		4	16	3	12	4	16	4	16
The machine will take up no more than 15 m^2 of floor area	6		4	24	4	24	3	18	2	12
The machine will not feature a robot arm	3		0	0	4	12	4	12	2	6
The machine will adhere to the british standards for fire, and health and safety executive	10		4	40	4	40	4	40	4	40
The machine will produce minimal waste materials	4		4	16	3	12	4	16	3	12
Machine components will be easily accessible for quality control and inspection	6		2	12	1	6	3	18	4	24
Material Handling will be minimised	3		4	12	1	3	2	6	3	9
Total Weighted Score			132		135		155		147	
Rank			4		3		1		2	

Table 4 compares methodically, using the MCDA method, how each concept performs against the selected criteria from the product design specification.

Table 4 shows that Concept 3 ranked highest among the four designs, making it a key influence in selecting the final concept. However, elements from other concepts also contributed to the final design, as shown in Figure 5.

Battery Module Assembly

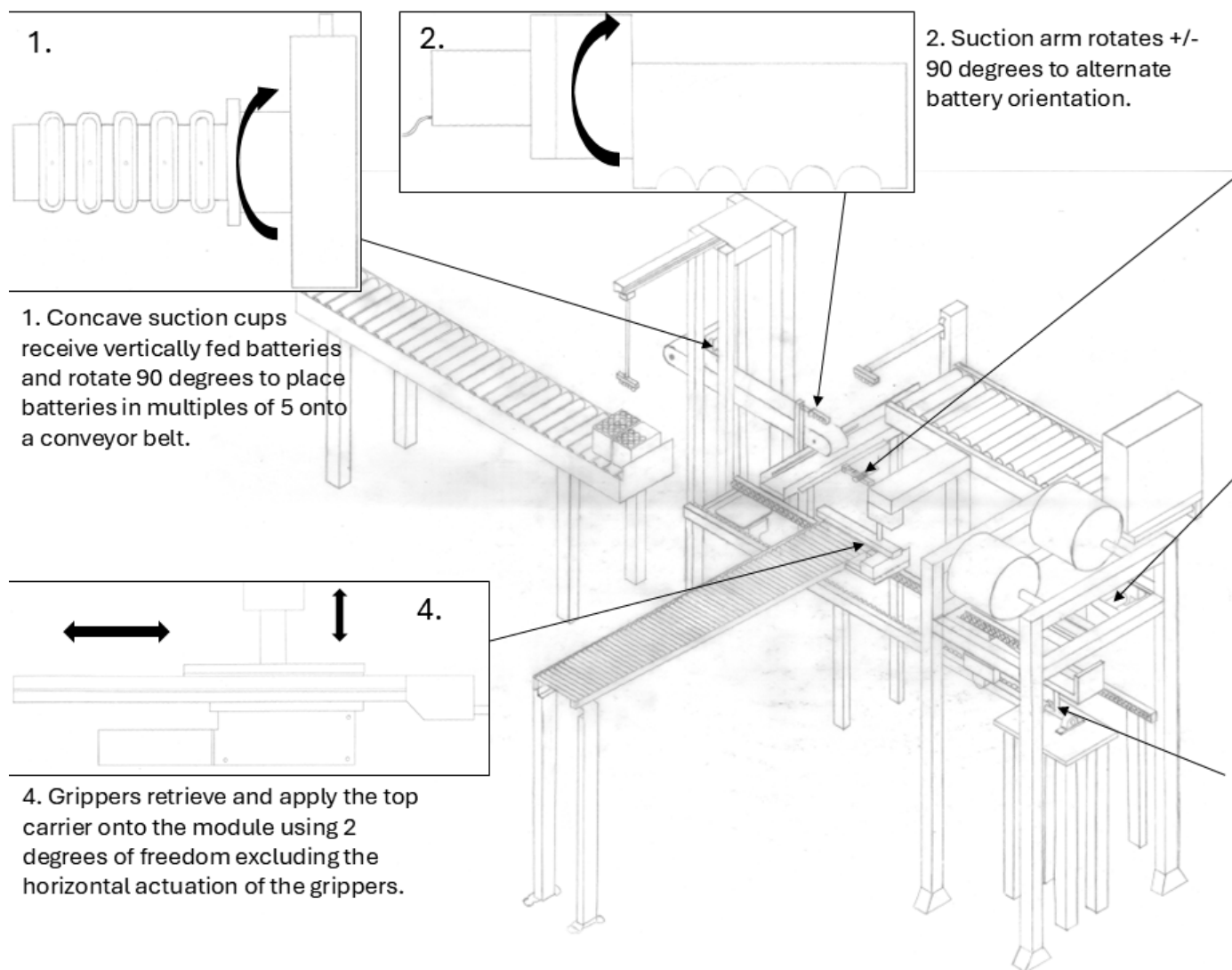


Figure 5 depicts the final machine design concept that draws upon aspects of all the initial concepts to produce a final machine.

Figure 5 shows how elements of each concept, and especially concept 3, are reflected on this final concept.

From Concept 1, the following has been retained:

- Rack and pinion mechanism

From Concept 2, the following have been retained:

- Battery conveyor buffer
- Module ejection conveyor

From Concept 3, the following have been retained:

- Vacuum suction cups
- Battery extraction method
- Battery rotation

Battery Module Assembly

- Top carrier application
- Central operations conveyor

From Concept 4, the following have been retained:

- Module rotation
- Copper strip application

While key elements from the initial concepts were retained, most ideas were refined to address identified issues. Each function was carefully evaluated, with many aspects evolving throughout the design process. For example, Function 3, shown in orthographic view in Figure 5, underwent significant changes in the final design, with certain steps removed to streamline material handling.

3.5 Component Calculations and Selection

Sub assembly 1: Battery Extraction Process

Custom L Plate:

This custom component connects a pneumatic rack and pinion motor to 5 concave suction cups such that they can be rotated 90 degrees onto the conveyor belt.

To check whether the connecting plate would withstand a suitable number of cycles before failure, the failure mode assessed in the following calculations is the fatigue stress of the interface with the actuator. This failure mode is suitable for this component because it handles minimal loads, therefore, assessing the buckling deflection or yield point of the plate would not be a suitable failure mode to analyse. Because the component is subject to thousands of cycles per day, the fatigue of the component is the best way to evaluate this part.

Assumptions:

- Fatigue exponent of aluminium is -0.12
- Ultimate tensile strength of Aluminium is 210 MPa
- Life cycle under 80% UTS is 1000 cycles

To calculate the moment applied by the actuator on the connecting plate, the moment of the plate, suction cups, level compensators, and solenoid valves is outlined in equation 1, and visualised in figure 6.

$$\begin{aligned}\sum \text{Moments} &= (5 \times 0.017 + 5 \times 0.085 + 5 \times 0.05 + 0.114) \times 9.81 \times 0.00186 \\ &= 0.016 \text{Nm}\end{aligned}$$

Equation 1 determines the sum of moments acting about centre of rotation of the connecting plate

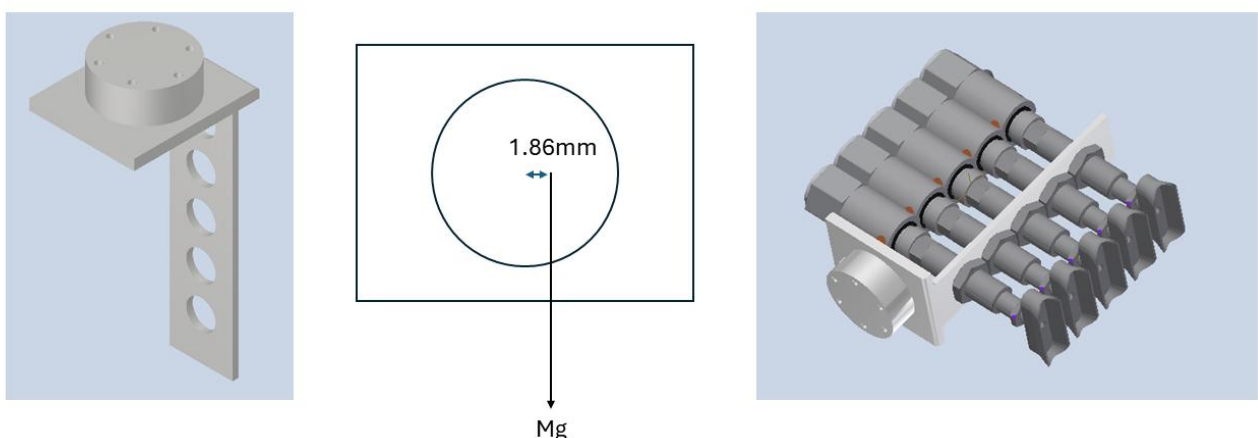


Figure 6 shows the custom plate with and without the suction cups it rotates to rotate the batteries. It also provides a free body diagram that helped in determining the moment about the centre of rotation of the actuator.

Battery Module Assembly

To find the maximum stress applied on the circular section of the connecting plate, the polar second moment of area for the interface between the actuator and the connecting plate is determined in equation 2.

$$J = \frac{\pi 0.04^4}{32} = 8.04 \times 10^{-8} m^4$$

Equation 2 outlines the method of obtaining the polar second moment of area of the circular section of the Custom L plate.

To determine the maximum torsional stress applied on the outermost section of the circular connection, equation 3 was used.

$$\tau_{max} = \frac{Tc}{J} = \frac{0.016 \times 0.02}{8.04 \times 10^{-8}} = 3,980 Pa$$

Equation 3 determines the maximum torsional stress applied on the outermost region of the circular connection to the actuator. 'c' is the radius of the circular connection.

The amplitude stress is determined from equation 4.

$$\sigma_a = \frac{\tau_{max}}{2} = 1,990 Pa$$

Equation 4 calculates the amplitude stress.

From the amplitude stress, the number of cycles before failure can be determined using the fatigue life prediction equation shown below:

$$\log(S) = b \log(N) + \log(C)$$

Equation 5 presents the fatigue life prediction equation where S and b are known values.

Before proceeding to determine the life cycle of the custom component, a boundary condition must be assessed to determine the value of $\log(C)$. This method is outlined in equation 6.

$$\log(0.8 \times 210) = 3b + \log(C)$$

$$\log(C) = 2.585$$

Equation 6 determines $\log(C)$ using the assumption that at 80% of its UTS, the material can undergo 1000 cycles.

Now that $\log(C)$ has been determined, we can find the total life cycle of the component using once again the fatigue life prediction equation.

$$\log(0.00199) = -0.12 \times \log(N) + 2.585$$

$$N = 10^{44}$$

Equation 7 shows the final calculation to determine the life cycle of the custom plate.

Battery Module Assembly

As such, the custom L plate will undergo 10^{44} cycles before failing. If approximately 1000 modules are produced every day and that therefore, the actuator rotates 26,000 times in a day, the component will theoretically last 3.84³⁹ years which is long enough.

Concave Suction Cups:

These concave suction cups are secured onto the custom L plate using level compensators to relay batteries from their vertical/upright position into their horizontal position such that they can be released onto the conveyor.

To determine the failure pressure of the cups to provide enough suction pressure to carry a Panasonic-NCR-18650B battery, the failure mode used to assess the suction cups was the adhesive failure mode. The adhesive failure mode determines whether the suction pressure provides enough force to support the weight of a battery. Adhesive failure is the correct failure mode to analyse for suction cups because the cup's ability to hold weight depends on the adhesive force generated by the suction pressure, which is the primary factor in detachment. Other failure modes like deflection or buckling are less relevant, as they do not significantly impact the cup's ability to maintain suction.

Assumptions:

- Safety factor of 1.5
- Coefficient of friction between the battery and the cup is high
- The weight of a battery is 0.47N

To calculate the adhesive failure of the suction cups, the contact area of the cup against the battery must be determined and is outlined in equation 8 and clarified from figures 7 and 8 as well as equation 9.

$$A = \theta r h = 2.02 \times 0.00915 \times 0.042 = 0.000776 \text{ m}^2$$

Equation 8 calculates the contact area between the suction cup and the battery.

Battery Module Assembly

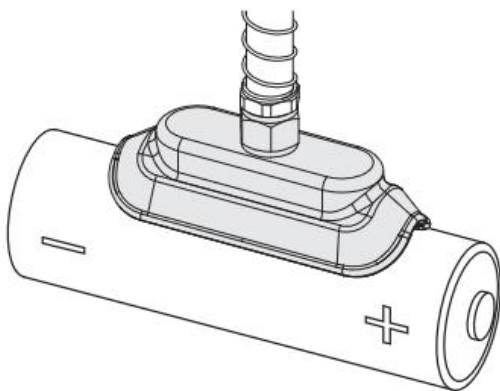


Figure 7 clarifies how the suction cup latches onto the battery and shows where equation 8 stems from.

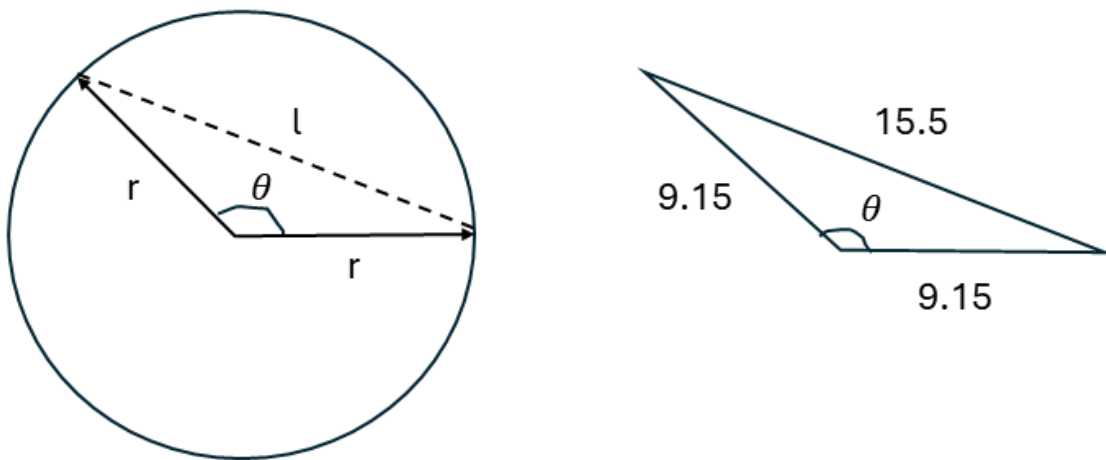


Figure 8 shows how the angle of contact, theta, was determined to find the contact area between the suction cup and the battery. Equation 9 clarifies how theta was mathematically determined.

$$\cos(\theta) = \frac{r^2 + r^2 - l^2}{2 \times r \times r}$$

$$\theta = 115.77^\circ = 2.02 \text{ rad}$$

Equation 9 leverages the cosine law to determine angle theta, 2.02 rad.

From these equations, we can apply equation 10 coupled with a safety factor to determine how much gauge pressure is required to grasp the batteries.

$$P = \frac{F \times N_d}{A} = \frac{0.47 \times 1.5}{0.000776} = 907 \text{ Pa}$$

Equation 10 calculates the required pressure to safely adhere to the batteries given a design factor of 1.5.

The adhesive failure mode occurs at 907 Pa. For the five concave suction cups that are mounted on the custom plate, a total of 4.54 kPa will have to be supplied.

Electric Slider Actuator:

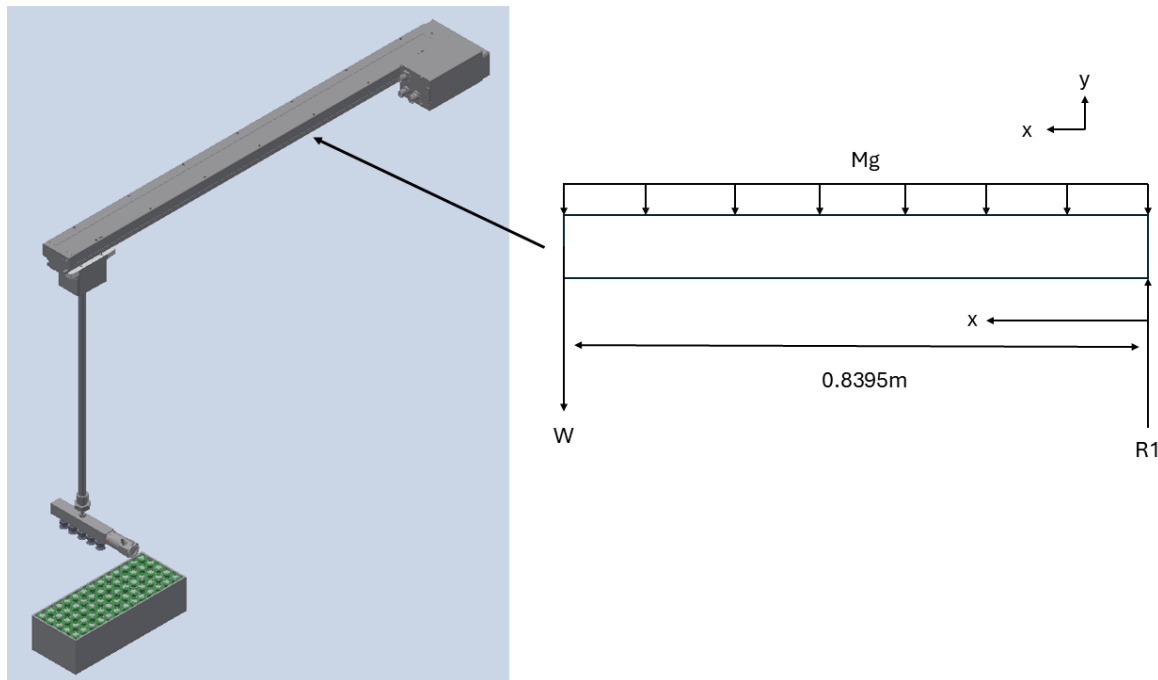
The electric slider provides the lateral movement of the batteries from their box to the concave suction cups.

To check whether the deflection of the electric slider actuator induces misalignment of the batteries with the suction cups, the failure mode assessed in the following calculations is the deflection of beams. This failure mode was assessed because for a cantilever beam aligning the suction cups to the batteries, a slight deflection could lead to misalignment in the picking of the batteries.

Assumptions:

- The actuator is entirely made of aluminium.
- The Young's Modulus of aluminium is 70 GPa.
- The actuator is modelled as cantilever beam.
- The cantilever beam is modelled as a rectangular cross section of $0.0376 \times 0.057\text{m}$
- Loads on the cantilever beam act at one end of the beam
- Reaction forces on the cantilever beam act at the other end of the beam
- Small angle approximations will be used
- A design factor of 3 will be used

To calculate the deflection of the beam a free body diagram must be initially considered, as can be seen from figure 9.



Battery Module Assembly

Figure 9 shows the configuration of the electric slider and how it was modelled as a cantilever beam on a free body diagram.

Considering two separate loads on the beam as a uniformly distributed load from the weight of the beam itself, and the point load W , equations 12 to 13 calculate the respective beam deflections.

$$I = \frac{b \times h^3}{12} = \frac{0.057 \times 0.0376^3}{12} = 2.52 \times 10^{-7}$$

Equation 11 determines the moment of inertia considering the assumption of modelling the actuator as a rectangular cross section.

$$\delta_W = \frac{W \times Nd \times L^3}{3 \times E \times I} = \frac{3.99 \times 3 \times 0.8395^3}{3 \times 70 \times 10^9 \times 2.52 \times 10^{-7}} = 0.13 \text{ mm}$$

Equation 12 calculates the deflection of the beam due to the point load W as shown on figure 9.

$$\delta_{Mg} = \frac{Mg \times Nd \times L^4}{8 \times E \times I} = \frac{42.00 \times 3 \times 0.8395^4}{8 \times 70 \times 10^9 \times 2.52 \times 10^{-7}} = 0.44 \text{ mm}$$

Equation 13 calculates the deflection of the beam due to the UDL Mg as shown in figure 9.

As such the total deflection of the beam is 0.576 mm. From this deflection, we can leverage figure 10 to determine the deflection at the point of contact between the batteries and the suction cups.

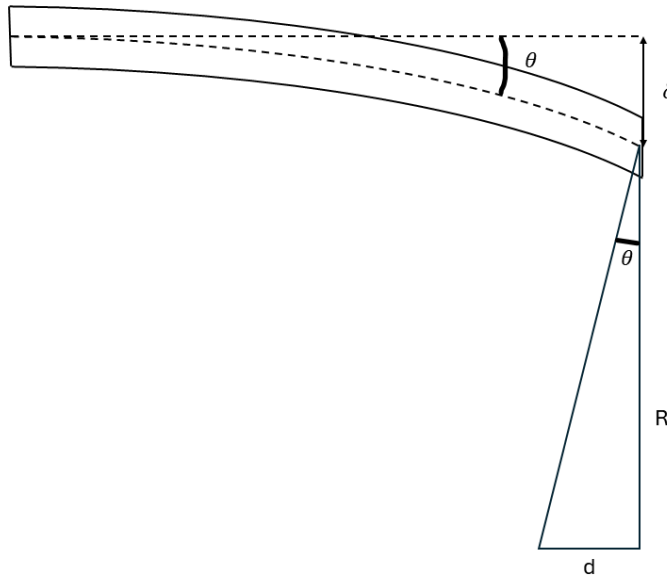


Figure 10 exaggerates the impact that the actuator deflection imposes on the battery pick up location.

Where $\delta = 0.63\text{mm}$, using equation 14 in conjunction with small angle approximation and coincident angles, this yields:

$$\theta = \left(\frac{\delta}{l}\right) = \left(\frac{0.000576}{0.8395}\right) = 0.000686 \text{ rad}$$

Equation 14 derives using small angle approximations, the angle theta.

Battery Module Assembly

Therefore, it can be shown from equation 15 that the overall deflection at the location of the batteries is 0.63mm.

$$R \times \tan(\theta) = 0.918 \times \tan(0.000686) = 0.63 \text{ mm}$$

Equation 15 determines the deflection d, as can be shown from figure 10.

The impact of the actuator deflection causes a displacement of 0.63mm at the location where the suction cups extract the batteries. This displacement is negligible and will not have an impact on the performance of the machine.

Sub assembly 2: Battery Insertion

The safety factor for all the calculations in sub assembly 2 was chosen to be 2.03 based on the design requirements of the sub assembly. This value was determined using equation 16 below.

$$N_y = \text{fatigue factor} \times \text{shock factor} \times \text{uncertainty factor} = b \times c \times d$$

Equation 16 determines the safety factor for an operation

The uncertainty factor was calculated using Pugsley's method as described in equation 17 below.

$$d = \text{operation factor} \times \text{seriousness of failure} = X \times Y$$

Equation 17 shows how the uncertainty factor was calculated using Pugsley's method

The fatigue factor was chosen to be 1.5 due to the cyclic loading of the part. The shock factor was chosen to be 1 as the forces applied to the parts were applied over a relatively long period of time. The uncertainty factor was determined to be 2.45 due to the simple loads experienced by the parts and the low risk to human life but the high economic risk. These factors combined to give the overall safety factor of 2.03.

Horizontal actuator:

The horizontal actuator was designed to connect the suction assembly that carries the batteries to the vertical actuator. This had the goal of moving the batteries laterally to the required position for pressing into the carrier.

To calculate the pressure required, the relationship between pressure, force and area was used. The failure mode for this part was the lack in pressure leading to the assembly not moving the desired amount.

In these calculations, it was assumed that there are no losses in pressure inside the actuator. Another assumption made was that there was no air resistance affecting the movement of the assembly.

Battery Module Assembly

To calculate the pressure required, a desired movement time was first chosen to be 1s. This value could then be used to calculate the required acceleration of the part with the known displacement of 0.295m as seen in equation 18 below.

$$a = \frac{2s}{t^2} = 2s = 2 \times 0.295 = 0.59ms^{-2}$$

Equation 18 calculated the acceleration required of the part

To determine the force required by the actuator the mass of the assembly calculated as shown below in equation 19.

$$m_{total} = 5 \times m_{battery} + 5 \times m_{suction\ cup} + m_{housing} = \frac{(5 \times 47.5) + (5 \times 4.5) + 73.94}{1000} \\ = 0.33kg$$

Equation 19 calculates the mass of the assembly at the end of the horizontal actuator

A free body diagram was constructed to show the force needed to be provided by the horizontal actuator seen below in figure 11.

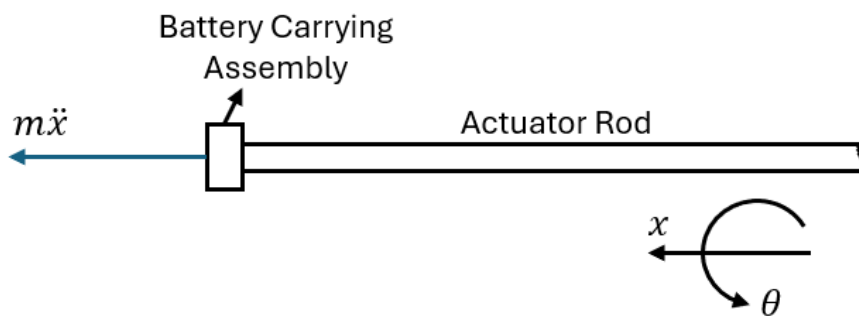


Figure 11 shows a free body diagram for the force required by the horizontal actuator

These values can then be used, alongside the safety factor, to calculate the force required by the actuator as shown in equation 20 below.

$$F = m_{total} \times a \times N_y = 0.40N$$

Equation 20 calculates the force required by the actuator

To calculate the pressure required to push the actuator, the cross-sectional area of the actuator rod was determined as shown in equation 21 below.

$$A = \pi r^2 = \pi \times \left(\frac{10}{1000} \right)^2 = \pi \times 10^{-4}$$

Equation 21 calculates the bore area of the actuator

Battery Module Assembly

These values can then be used to calculate the pressure required by the actuator shown below in equation 22.

$$P = \frac{F}{A} = \frac{0.40}{\pi \times 10^{-4}} = 1.3kPa$$

Equation 22 calculates the pressure required to move the actuator

This indicates that to move the assembly by $0.295m$ in $1s$, approximately $1.3kPa$ of pressure would be needed.

Another requirement of this actuator was ensuring that it did not overly deflect under the load at the end of the actuator such that the tolerance on the insertion of the batteries would be met.

To determine if the material would be deflecting an acceptable amount, equations using Macauley's notation were used. The failure mode for this requirement was the insertion of the batteries exceeding the maximum angular tolerance of 0.5° .

It was assumed that the centre of mass was at the midway point of the rod. This is a reasonable assumption as the mass at the end of the rod would be small in comparison to the mass of the overall rod. It was also assumed that the rod acted as a simply support beam with point loads applied. Also, a value for the Young's Modulus of aluminium was taken as $90GPa$

The first stage of determining the bending moment was creating a free body diagram system of the rod as shown below in figure 12.

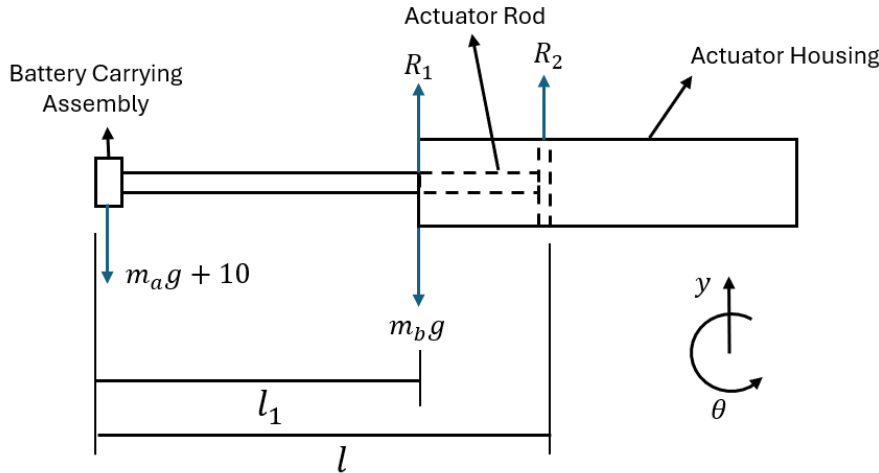


Figure 12 showing a free body diagram of the horizontal actuator

This free body diagram could then be used to calculate the reaction forces provided by the rod exit and the base of the rod. These can be seen below leading to equation 23.

$$\text{From FBD: } (m_{assembly} + m_{body})g = R_1 + R_2$$

Battery Module Assembly

$$\text{Moments about } O: m_a g l_1 + R_2(l - l_1) = m_b g \frac{l}{2}$$

$$R_2 = \frac{g \left(m_b \frac{l}{2} - m_a l_1 \right)}{l - l_1}$$

$$R_1 = (m_a + m_b)g - \frac{g \left(m_b \frac{l}{2} - m_a l_1 \right)}{l - l_1}$$

Equation 23 gives the equations used to calculate the reaction forces

Substituting values gives: $R_1 = 4.14N$ and $R_2 = 0.182N$ (3s.f.)

These reaction forces can be used to create an equation using Macaulay's notation to quantify the shear forces inside the rod as seen below in equation 24.

$$v = 0.182\langle x \rangle^0 - 0.981\langle x - 0.174 \rangle^0 + 4.14\langle x - 0.182 \rangle^0$$

Equation 24 describes the loads on the rod using Macauley's notation

This equation can then be integrated to find the bending moments, slopes and deflections inside the beam as shown in equation 25 below.

$$M = \int v \, dx = 0.182\langle x \rangle^1 - 0.981\langle x - 0.174 \rangle^1 + 4.14\langle x - 0.182 \rangle^1$$

$$\theta = \frac{1}{EI} \int M \, dx = \frac{1}{EI} [0.091\langle x \rangle^2 - 0.491\langle x - 0.174 \rangle^2 + 2.07\langle x - 0.182 \rangle^2 + C\langle x \rangle^0]$$

$$v = \int \theta \, dx = \frac{1}{EI} [0.03\langle x \rangle^3 - 0.164\langle x - 0.174 \rangle^3 + 0.69\langle x - 0.182 \rangle^3 + C\langle x \rangle^1 + D\langle x \rangle^0]$$

Equation 25 gives the equation for the deflection of the beam

Using the known boundary conditions of no deflection at $x = 0$ and $x = l - l_1$, the constants of integration can be determined as shown below.

$$\text{At } x = 0, v = 0 \Rightarrow D = 0$$

$$\text{At } x = l - l_1, v = 0 \Rightarrow 0 = 0.03\langle 0.182 \rangle^3 - 0.164\langle 0.008 \rangle^3 + C\langle 0.182 \rangle$$

$$C = -9.9 \times 10^{-4} \cong -0.001$$

Equation 26 calculates the constants of integration

These boundary conditions can be used in the completed deflection equation to give the deflection at the end of the rod as shown below.

$$v(x) = \frac{1}{EI} [0.03\langle x \rangle^3 - 0.164\langle x - 0.174 \rangle^3 + 0.69\langle x - 0.182 \rangle^3 - 0.001\langle x \rangle^1]$$

$$v(l) = v(0.348) = 4.17\mu\text{m}$$

Battery Module Assembly

Equation 27 shows the deflection equation being used to find the deflection at the end of the rod

This shows that a displacement of $4.17\mu m$ will be created at the end of the actuator rod which is negligible and so would not generate any significant misalignment of the batteries.

Vertical actuator

This part connects onto the end of the horizontal actuator such that the batteries can be inserted into the carrier with a pressing force of $10N$.

Method: To calculate the pressure required, the relationship between pressure, force and area alongside a free-body diagram was used. The failure mode for this part was the lack in pressure leading to the actuator not providing sufficient force.

The first stage of calculating the pressure was making a free body diagram to see all the forces acting on the body as seen below in figure 14.

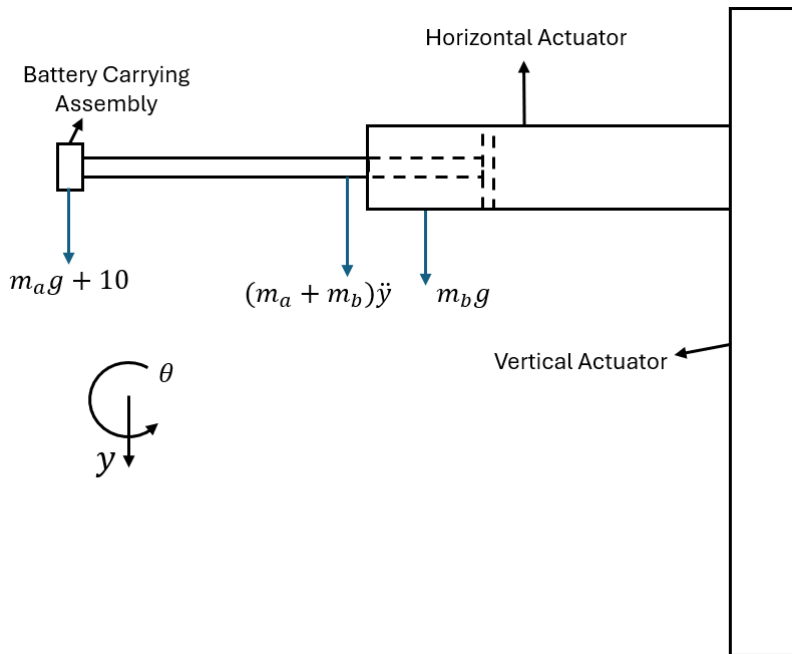


Figure 13 showing a free body diagram for the vertical actuator

The movement time for the actuator was chosen to be $2s$ which, when considering the displacement of $0.295m$, gives the total force shown in equation 28 below.

$$F = \left((m_a + m_b)g + \frac{(m_a + m_b)s}{2} + 10 \right) \times N_y = \dots = 21.02$$

Equation 28 calculates the force required by the actuator

After this, the area of the bore could be calculated using equation 19. This value could then be used alongside the force calculated in equation 29 to calculate the pressure as shown by equation 20. The final pressure calculation can be seen below.

Battery Module Assembly

$$P = \frac{F}{A} = \frac{21.02}{1.97 \times 10^{-4}} = 1.1Bar$$

Equation 29 calculates the pressure required by the actuator to provide the 10N insertion force

This shows that a pressure of 1.1Bar will be needed to move the vertical actuator so that a 10N insertion force can be actuated.

Electric motor

The electric motor was used to rotate a pinion gear to use a rack to move an assembly in the vertical direction. The amount of vertical movement required by this motor is equal to 2 revolutions. The time taken for this rotation to complete must be calculated so that the time needed by the overall subassembly could be calculated.

To find this time, a relationship between input and output torque and angular velocity was used to calculate the output angular velocity. The failure mode for this part was the rotation occurring too slowly and bottlenecking the rest of the subassembly.

It was assumed that the load was distributed evenly between all 4 motors. This is a reasonable assumption due to the even spacing of the motors. Further, it was assumed that the motor perfectly transmitted torque to the pinion gear with no mechanical losses.

A diagram illustrating these values in the system used is shown below in figure 14.

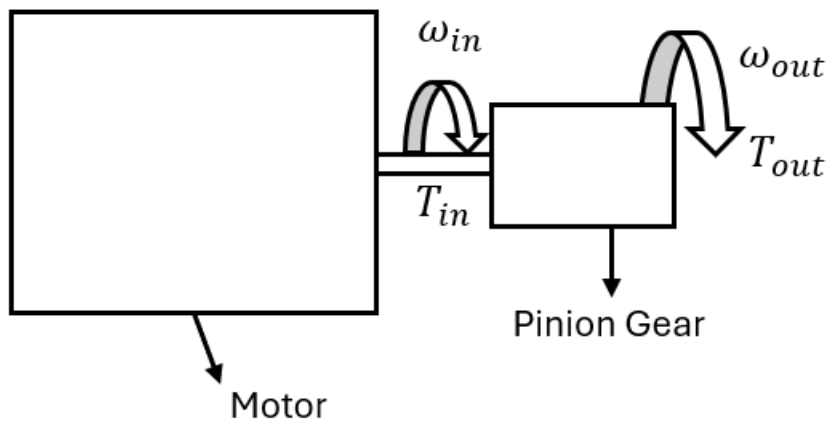


Figure 14 depicting a diagram of how the torque is transmitted between the motor and pinion gear

To determine the output torque required by the motor, equation 30 seen below was used.

$$T = Fr = mgr = 0.0690 \times 9.81 \times 0.065 \times Safety\ Factor = 89.30mNm$$

Equation 30 shows the output torque needed by the pinion motor to move the rack

Since the input torque and angular velocity are known from the motor selection, the output angular velocity can be calculated using equation 31 below.

Battery Module Assembly

$$\omega_{out} = \frac{T_{in}\omega_{in}}{T_{out}} = \frac{100 \times 279.25}{89.30} = 312.7 \text{ rads}^{-1} = 2986 \text{ rpm}$$

Equation 31 calculates the output angular velocity of the pinion gear

This speed in revolutions per minute could then be used to calculate the time needed for 2 revolutions as seen below.

$$t = \frac{2}{\text{rpm}} = \frac{2}{2986} = 0.04$$

Equation 32 determines the time required for the pinion gear to rotate 2 revolutions

This shows that the pinion gear will take 0.04s to rotate 2 revolutions making the time taken to lower and raise the suction assembly the same value.

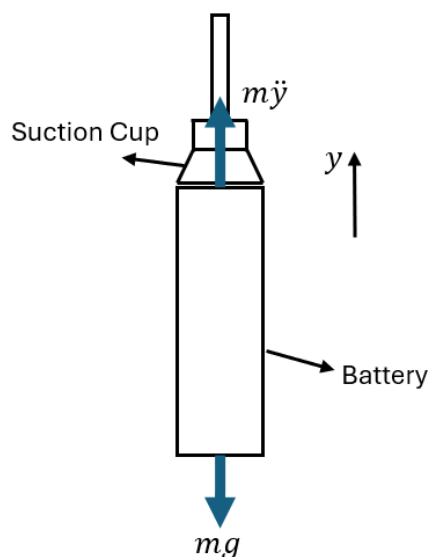
Vertical grabbing suction cups

The vertical grabbing suction cups are design to lift or lower the batteries in an upright position. For this, they needed to have sufficient pressure to lift the batteries without them falling.

To calculate this pressure required, a free body diagram of the system was constructed. This was then used to find the suction force required by a suction cup which was then used to find the pressure required. The failure mode for this part was the suction being insufficient and the battery not being able to be held.

For these calculations, it was assumed that the suction cups make an even contact with the batteries so that the contact area is the area of the internal circle. Additionally, it was assumed that the contact between the suction cup and the battery forms a tight lip seal around the edge.

The free body diagram for this system is shown in figure 15 below.



Battery Module Assembly

This free body diagram could then be used to calculate the pressure force required by a suction cup as shown in equation 33 below.

$$F = mg \times N_y = \left(\frac{48.81}{1000} \times 9.81 \right) \times 2.03 = 0.97N$$

Equation 33 showing the calculation for the force required by the suction cups

The next stage was to find the area of the suction cup as shown in equation 34 below.

$$A = \pi r^2 = \pi \times \left(\frac{7.75}{1000} \right)^2 = 1.9 \times 10^{-4} m^2$$

Equation 34 calculates the contact area between the suction cup and the battery

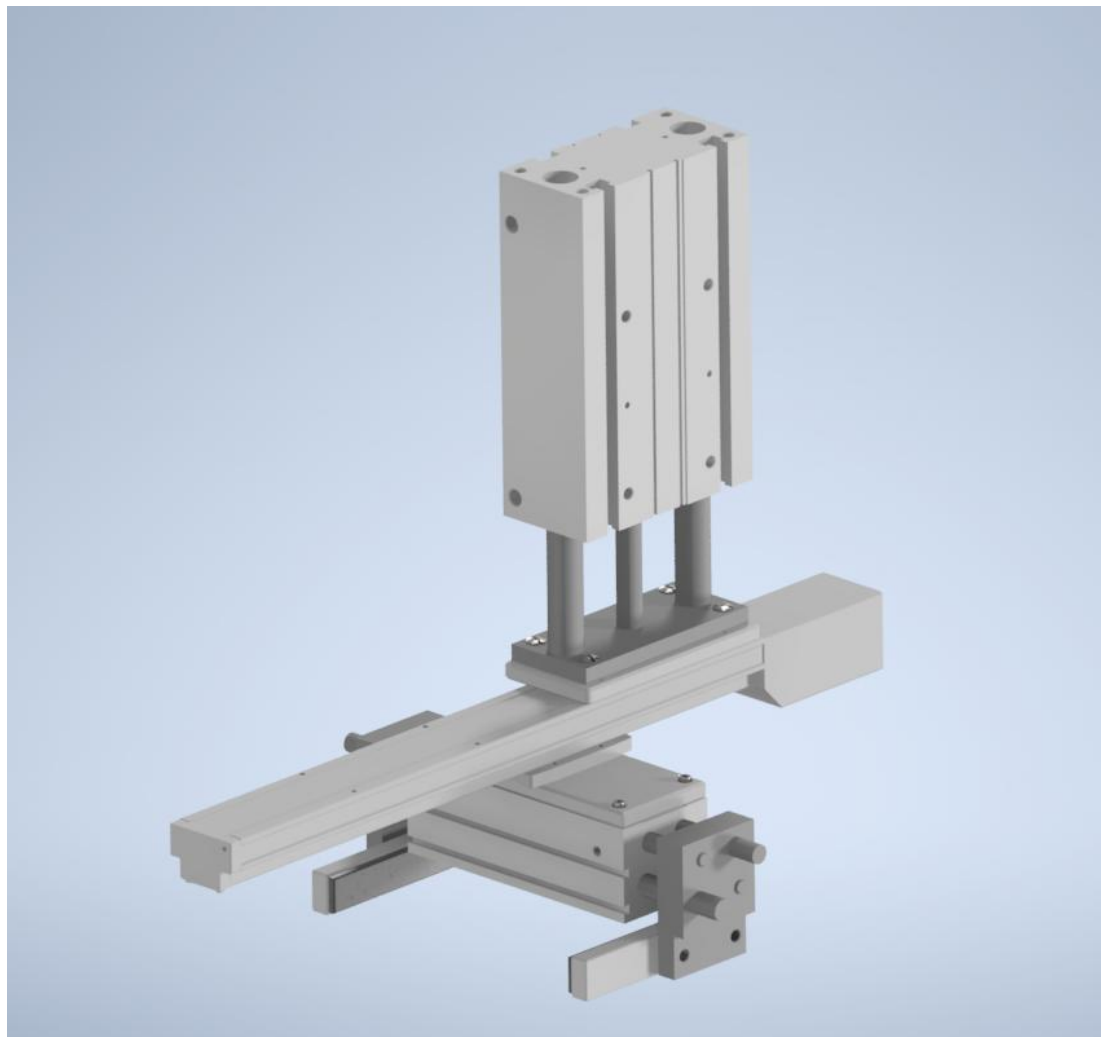
These could then be combined to find the pressure required by a suction cup as shown in equation 35 below.

$$P = \frac{F}{A} = \frac{0.97}{1.9 \times 10^{-4}} = 5.2kPa$$

Equation 35 determining the pressure required by a suction cup to lift a battery

This gives the pressure required by a single suction cup to lift a battery as $5.2kPa$. Since the subassemblies using the suction cups utilise 5 at a time, one of these subassemblies would require $26kPa$ of pressure.

Sub-Assembly 3: Top Carrier Application



Component	Mass (kg)	Force (N)
Electric Actuator (LEFS25-400mm)	4.95	48.56
Pneumatic Actuator (MGPM63TF-200Z)	8.37	82.06
Gripper (MLH32)	4.8	47.09
Adapter Plates	0.623	6.11
Top Carrier	0.16	1.57
Total	18.91	185.44

Table 5 breaks down the components of sub assembly 3 to perform accurate calculations later.

Beam Load, Bending Stress & Deflection Check

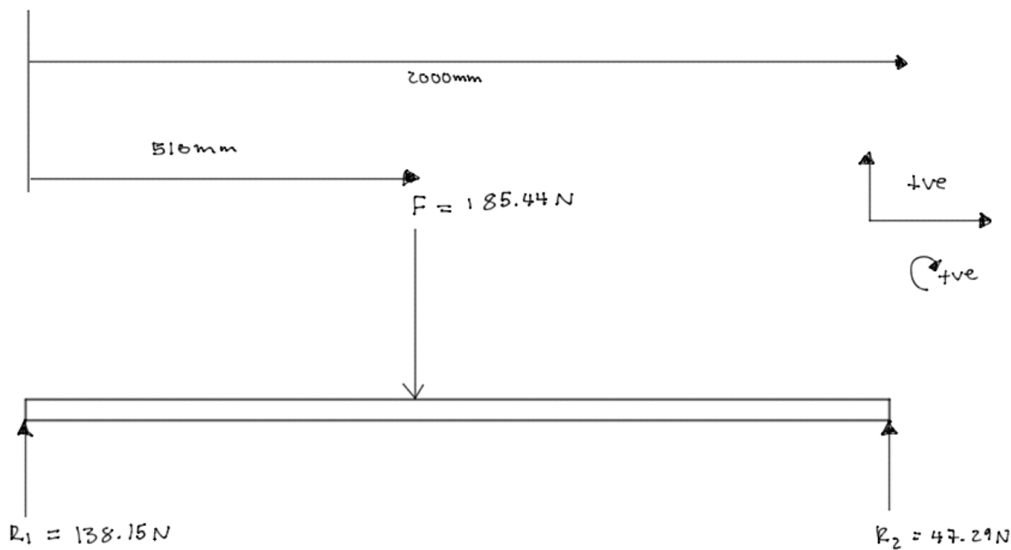


Figure 15 depicts the free body diagram for an aluminium support beam.

To check whether the horizontal aluminium support beam ($160 \times 80 \text{ mm}$) would deflect excessively under the weight of the suspended upper carrier sub-assembly. The beam was modelled as a simply supported beam with a point load applied off-centre at a distance of 510 mm from the left support, as seen in Figure 11. This setup represented a conservative approach because real-world profile end fixings would have reduced bending and supported stiffness.

Assumptions/Parameters:

- Beam length: 2.0 m
- Point load: 185.44 N
- Load location: 510 mm from one support
- Beam material: Aluminium 6061-T6
 - $E = 69 \text{ GPa}$
 - $\sigma_y = 95 \text{ MPa}$
- Moment of Inertia $I = 2.45 \times 10^{-7} - 7 \text{ m}^4$
- Section modulus $Z = 2.45 \times 10^{-5} \text{ m}^3$, $a = 0.51$, $b = 1.49\text{m}$

$$\delta = \frac{Fab^2}{3EIL} = \frac{185.44 \cdot 0.51 \cdot (1.49)^2}{3.69 \times 10^9 \cdot 2.45 \times 10^{-7} \cdot 2.0} = 2.07\text{mm}$$

Equation 36 determine the deflection of a simply supported beam for a given point load.

Battery Module Assembly

This is acceptable. The bending stress is significantly lower than the yield strength (safety factor SF ≈ 33), and deflection is well below the common serviceability threshold of $L/250 = 8\text{mm}$.

Vertical Actuator Forces (MGP63TF-200Z)

To check whether the selected pneumatic actuators (MGP and MLH series) can safely lift and hold the upper carrier sub-assembly under vertical loading. Each actuator was treated as a cylinder applying vertical force under gauge pressure, where total available force was calculated by:

$$F = P \cdot A$$

Equation 37 displays the relationship between force pressure and area.

This was compared to the weight of the load to check for sufficient lifting capacity, assuming vertical motion only.

Assumptions/Parameters:

- Operating pressure: 0.4 MPa
- MLH32: bore = 32 mm : $A = 804.25\text{mm}^2$
- MGP63: bore = 63 mm : $A = 3117.25\text{mm}^2$
- Force from MLH: $F = 0.4 \times 10^6 \times 804.25 \times 10^{-6} = 321.7 \text{ N}$
- Force from MGP: $F = 0.4 \times 10^6 \times 3117.25 \times 10^{-6} = 1246.9 \text{ N}$
- Total available force: $1,568.6 \text{ N}$
- Weight of full vertical sub-assembly: 103.33 N

Total actuator force \gg weight of assembly with an SF of 15.17. This is more than sufficient. The selected actuators can easily lift and hold the full assembly with a large margin, ensuring reliable operation under all normal loads. Control and stability are also likely to be good given the vertical orientation and overcapacity.

Gripper Forces (MLH32):

To check whether the MLH32 pneumatic gripper could securely grip and hold the top carrier without slipping during horizontal motion,

The required holding force was calculated by taking the gravitational force on the top carrier and dividing it by the coefficient of friction between the rubber pads and the aluminium carrier surface. The calculation assumed two contact points (fingers) apply normal force symmetrically, and slip occurred horizontally.

Assumptions/Parameters:

- Gripper: MLH32
- Bore diameter: 32 mm → area per finger: $A = 804.25\text{mm}^2$
- Operating pressure: 0.4 MPa
- Normal force (total from both fingers):

$$F = P \cdot A = 0.4 \times 10^6 \times 804.25 \times 10^{-6} = 321.7\text{N}$$

- Coefficient of friction (rubber on aluminium): $\mu = 0.6$
- Gripping force available from friction:

$$F_{friction} = \mu \cdot F = 0.6 \times 321.7 = 193.02\text{N}$$

- Top carrier weight: 1.57 N

$$F = m \cdot a = 0.16 \cdot \frac{v^2}{2s} = 0.16 \cdot o. \frac{5^2}{2 \cdot 0.33} \approx 0.06\text{N}$$

The MLH32 gripper generated a total normal force of 321.7 N at 0.4 MPa operating pressure. With a coefficient of friction of 0.6, this results in a maximum frictional holding force of 193.02 N. The top carrier weighs 0.16 kg, requiring only 1.57 N to support it against gravity. Even under dynamic acceleration from 0 to 0.5 m/s over a 330 mm stroke, the estimated inertial force is 0.06 N. The resulting safety factor exceeds 120, confirming the gripper provides more than sufficient force to hold the carrier securely during all phases of motion.

Vertical Pneumatic to Electric Horizontal Actuator Bolt Stress Analysis

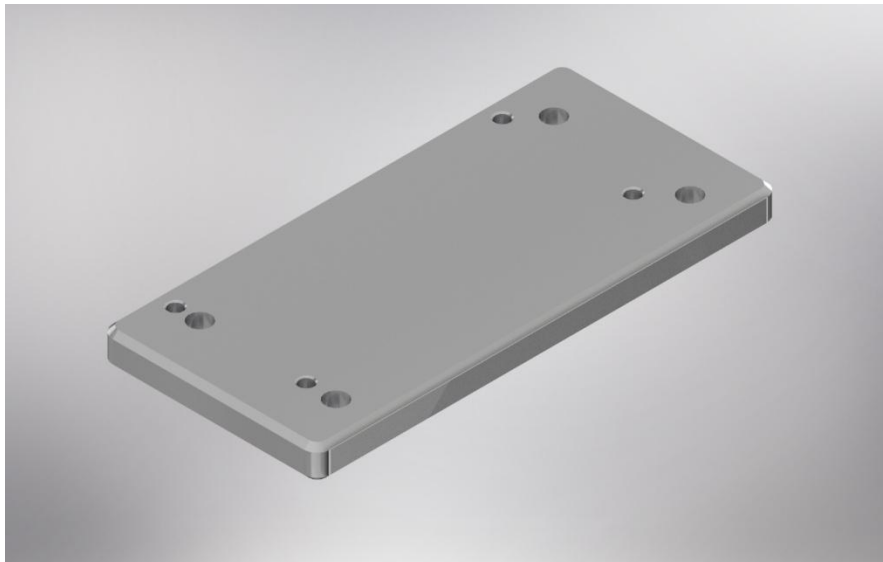


Figure 16 shows an image of the custom component whose failure mode will be analysed shortly.

To ensure the $4 \times M8$ bolts used to connect the adapter plate to the vertical actuator can withstand the vertical load applied by the full upper sub-assembly without yielding. Each bolt was modelled as carrying an equal share of the vertical load in tension, assuming standard core diameter for M8 fasteners. The tensile stress was calculated using:

$$\sigma = \frac{F}{A}$$

and compared to a conservative estimate for the yield strength of steel (400 MPa).

Assumptions/Parameters:

- Total vertical load: 177.6 N
- $4 \times M8$ bolts (standard)
- Core diameter of M8 bolt: 6.466 mm
- Area: $A = 3.28 \times 10^{-5} m^2$
- Force per bolt: $\frac{177.6}{4} = 44.4 N$
- Steel yield strength: 400 MPa

Each M8 bolt experiences only 1.35 MPa of tensile stress, which is minimal compared to the assumed yield strength of 400 MPa. This results in a very high SF of 296, confirming that the bolts can comfortably support the 177.6 N vertical load from the sub-assembly.

Battery Module Assembly

The connection is highly secure under normal operating conditions, with ample margin against failure.

Sub assembly 4: Copper strip Application

Module Gripper:

Required a gripper head that could grip module along the short side and so needed a gripper head which would span the longer side. This side had a length of 270.44mm but the gap between the fingers would need to widen past this slightly.

Total stroke	- -	260 10.24		[mm] [inch]
Grip width range *	170 6.69	-	430 16.93	[mm] [inch]

Table 1 6: Gripper Datasheet

The OnRobot 2FGP20 has a minimum grip width range of 170mm and a maximum grip width of 430mm so it matches the requirements comfortably.

Motors and Gearheads:

3 motors total were required for the copper strip application sub assembly. There were 2 distinct functions which required motors, and a different gearhead was used for each function. The first was the 90° angular rotation of the gripper arm which would position the module into the upright position and this function only required 1 motor. The second required 2 motors and these drove tape rollers which aligned the copper strips in front of the module.

At the bottom of the gripper arm is a shaft which connects to the motor and gearhead. It was decided that a Maxon motor would be used. The selection guidelines set out by the supplier are given as a series of steps. The motor and gearhead for the first function was selected first. The steps were followed as shown:

Battery Module Assembly

Step 1: Situation Overview

The FBD below shows the basic dimensions of the drive shaft, arm and gripper:

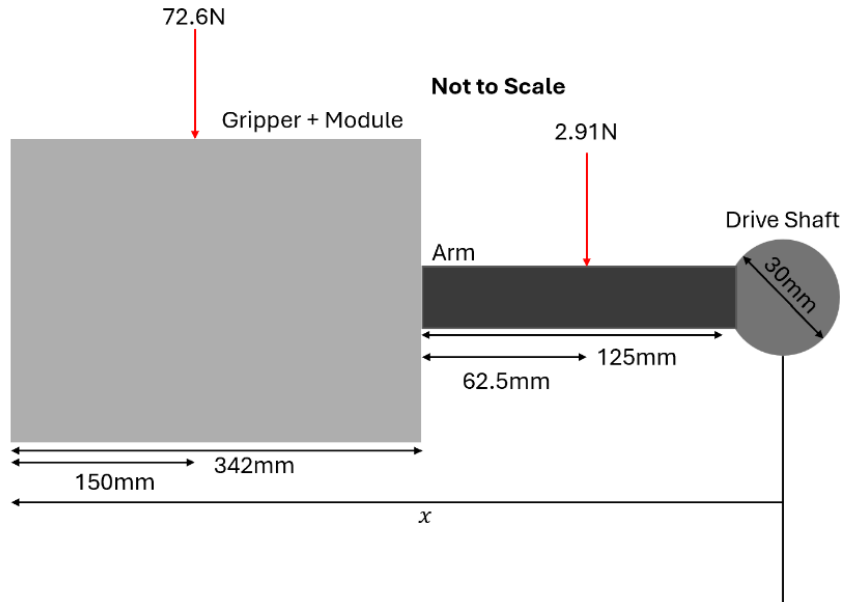


Figure 17: FBD of Gripper Arm + Module

With some assumptions the torque on the drive shaft can be calculated.

Step 2: Load

The forces on the FBD are approximated from the 2FGP20 data sheet, and weight estimations for the battery module and arm. The centre of gravity for the module + gripper is an estimation.

$$\begin{aligned} \text{Arm Weight: } L * W * \text{Height} * \text{Al density} * 9.81 &= \text{Weight} \\ &= 0.04 * 0.125 * 0.022 * 2700 * 9.81 = 2.91N \end{aligned}$$

$$\text{Module + Gripper} = 4\text{kg} + 3.4\text{kg} * 9.81 = 72.6N$$

The torque acting on the drive shaft can be calculated with the equation:

$$T = Fx$$

$$T = (2.91 * 77.5 * 10 - 3) + (72.6 * 332 * 10 - 3)$$

$$T = 24.3Nm$$

Equation 38 determines the torque required for the gripper arm.

And so the output torque after gearhead reduction had to be at least 24.3Nm.

Step 3: Motor Selection

Because there are gearheads with numerous gear ratios, the actual torque output of the motor was not the biggest consideration. Rather elements such as brushes, bi-directionality and controller compatibility took precedence. The EC-i 40 Ø40 mm, brushless, 100-Watt servomotor was selected. The lack of brushes ensured longevity which is key to the repeated back and forth rotation of the arm.

Step 4: Gearhead Selection

The motor has a load speed of 4390 RPM which when reduced through the selected Planetary gearhead GPX 42 UP Ø42 mm, 4-stage (546:1) results in an 8 RPM output which means a 90 ° rotation would occur in 1.87 seconds which is acceptably fast but not so fast that the module could fall out of the gripper. Additionally, this gearhead is rated for 35Nm which is well above the 24.3Nm required giving a safety factor of about 1.3

The motor selected for the first function was repurposed for the second however a smaller torque was required for the copper strip rollers and so a Planetary gearhead GPX 42 UP Ø42 mm, 4-stage with a gear ratio of (113:1) was used this time.

Custom Gripper Arm:

The custom gripper arm is a key component of the system which connects the motor to the gripper. As seen in the FBD above it carries a significant amount of load. The goal was to determine the fatigue life of the gripper arm under cyclic loading and assess when it is likely to fail.

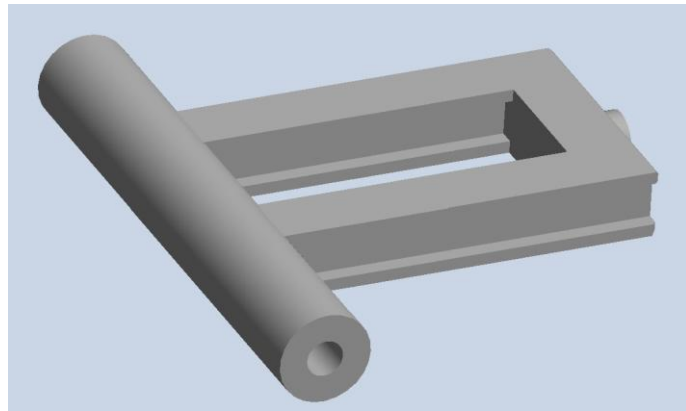
Assumptions:

- The arm behaves as a cantilever beam
- Material is Aluminum 6061-T6
- Slope of the fatigue curve (b) was assumed to be -0.09
- A fatigue strength (S) of 96 MPa for 10^7 cycles

To calculate stresses, we consider the FBD already used in the motor calculations.

Below is a visual of the component itself:

Battery Module Assembly



For a more accurate estimation of fatigue life, we must look at the cycles the arm undergoes. During the production of one module, the arm experiences 2 cycles without a module attached to the gripper and 2 without. By taking the average of the load induced in both situations the accuracy of the estimation increases:

For maximum load:

$$M_{Loadmax} = F_{Loadmax} \times L$$

Which comes out to:

$$72.5 \times 0.125 = 9.06Nm$$

And for minimum load:

$$33.3 \times 0.125 = 4.16Nm$$

With the 2 bending moments calculated, both stresses could also be calculated but first the second moment of area (I) had to be found for the I beam:

$$\frac{1}{12} \times (bh^3 - b_w h_w^3)$$

$$I = 1.546 \times 10^{-8} m^4$$

The bending stress formula is:

$$\sigma = \frac{Mc}{I}$$

$$\sigma_{max} = 6.45MPa \text{ and } \sigma_{min} = 2.46MPa$$

The mean and alternating stresses are given by:

$$\sigma_m = \frac{\sigma_{max} + \sigma_{min}}{2}, \sigma_a = \frac{\sigma_{max} - \sigma_{min}}{2}$$

And their values found to be $\sigma_m = 4.705MPa$ and $\sigma_a = 1.745MPa$

Battery Module Assembly

We can now use the fatigue life prediction equation to estimate fatigue life in terms of cycles:

$$\log(S) = b \log(N) + \log(C)$$

Rearranging for N , the number of cycles we get:

$$N = 10^{\frac{\log(S)-\log(C)}{b}}$$

$$N \approx 2.09 \times 10^{12} \text{ cycles}$$

Even with a high initially estimated cycle rate of 4424 cycles per day, the custom arm is at very low risk of failure and likely is a component that will never need to be replaced.

Bearings:

HPC 30mm Pillow Block bearings provided a simple method of mounting shafts. They are mountable on both flat horizontal and vertical surfaces which was useful for this sub-assembly where the arm shaft required horizontal mounting and the large tape rollers required vertical.

Actuators:

300mm was required and the other 200mm. The DSNU-50-320-PPV-A and DSNU-40-200-PPV-A actuators were selected under the assumption that the strips only had to contact the battery heads with no additional force required. The mass of the block the actuators were moving was $1.8kg$ so a minimum force of $17.66N$ was required. However, in order to have fast movement and additional force to ensure the strip was actually cut, extra pressure equivalent to $5N$ was added. Using the equation for pressure in terms of force and area, the required bar could be calculated for both actuators. The time taken for press was estimated.

$$P = \frac{F}{A}$$

$$P = \frac{22.66}{2.0106 \times 10^{-4}}, \frac{22.66}{1.131 \times 10^{-4}}$$

$$P = 1.12 \text{ bar}, 2 \text{ bar}$$

Battery Module Assembly

The actuator specs given by Festo states an operating pressure range of 1-10 bar, so these values are ideal:

Operating pressure	0.1 MPa ... 1 MPa
Operating pressure	1 bar ... 10 bar
Mode of operation	Double-acting
Operating medium	Compressed air to ISO 8573-1:2010 [7:4:4]

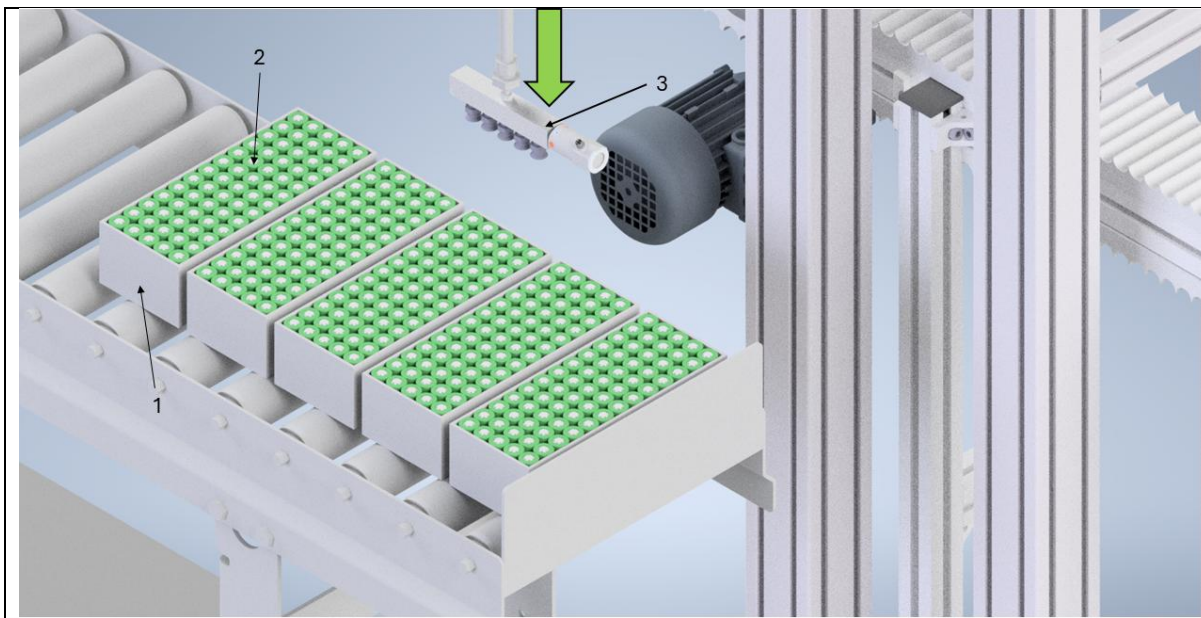
Table 7: Actuator Datasheet

It is estimated that with the right tubing and flow rate of 20 L/min a stroke velocity of 1 m/s would be achievable.

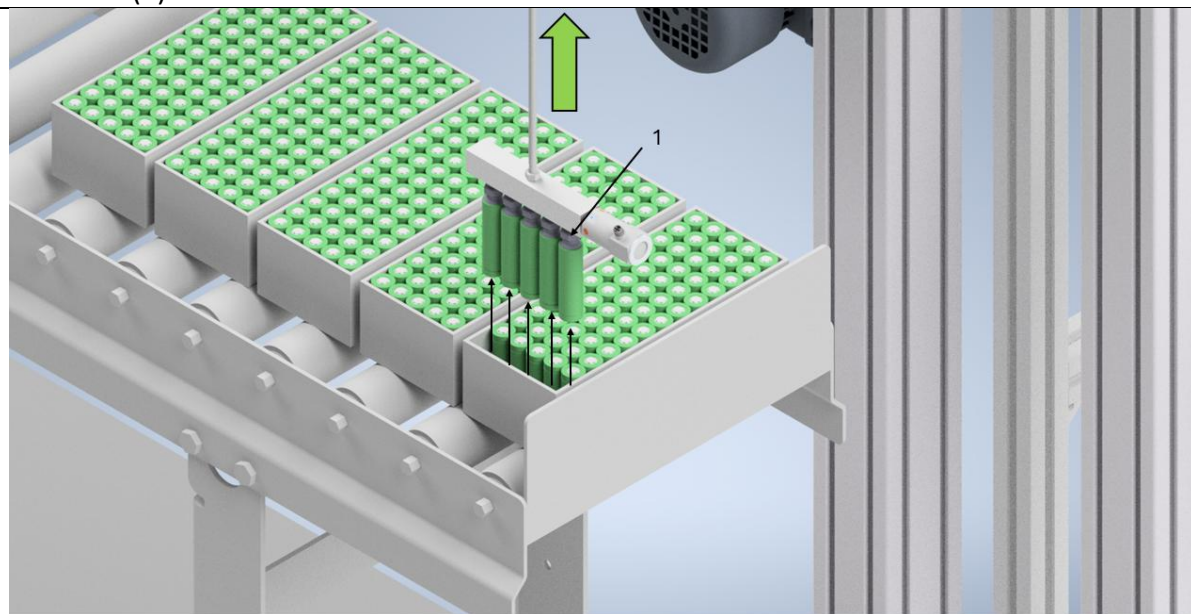
Pressure Sensors:

The D-M9P is a pressure sensor mounted onto both actuators which will be wired into the PLC ensuring the press block consistently moves the same distance for each stroke. They are used for signalling when the press block reaches the module surface for control purposes.

3.6 Method of Operation Storyboard

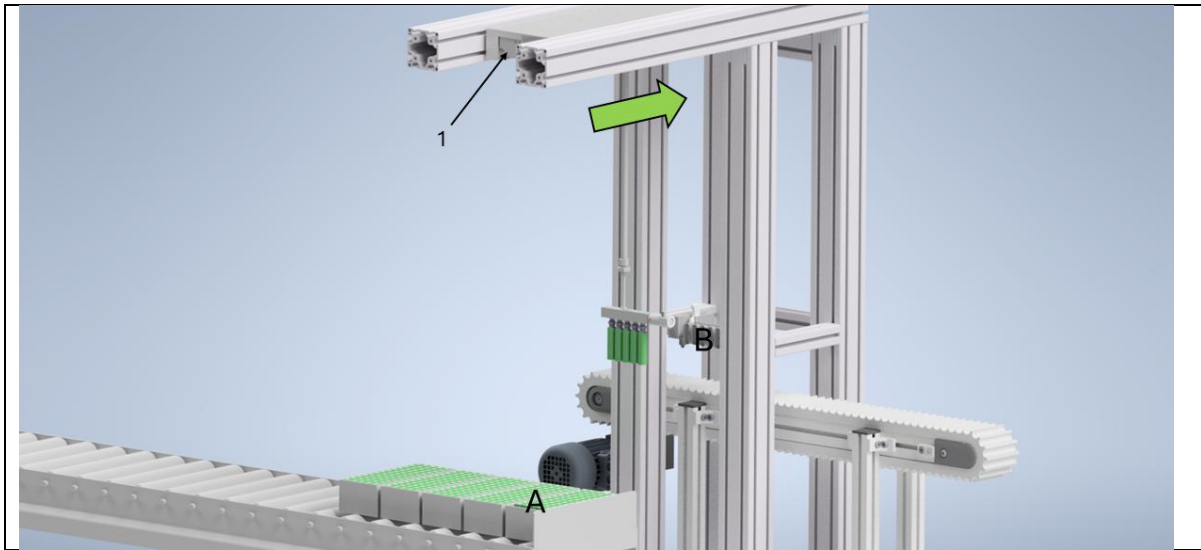


The battery boxes (1) are buffered on roller conveyor. A linear pneumatic actuator (3) travels vertically downwards until it has moved out by 333mm and made contact with the batteries (2).

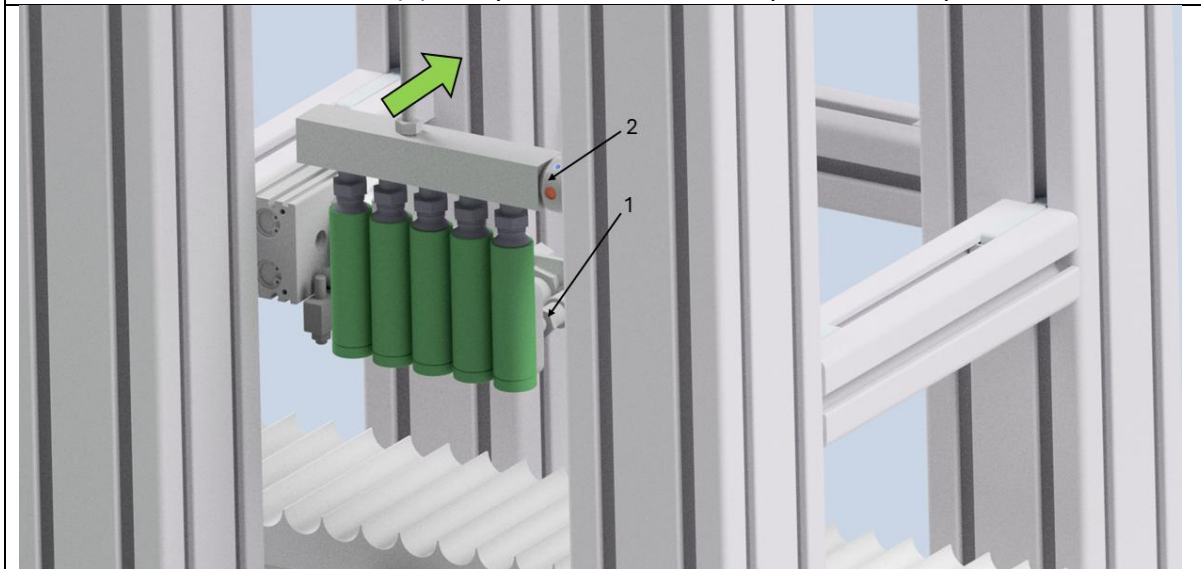


As the suction cups (1) make contact with the batteries, the solenoid valve generates a loss of 15kPa. This causes the batteries to suck to the cups. The actuator then moves back to its original height.

Battery Module Assembly

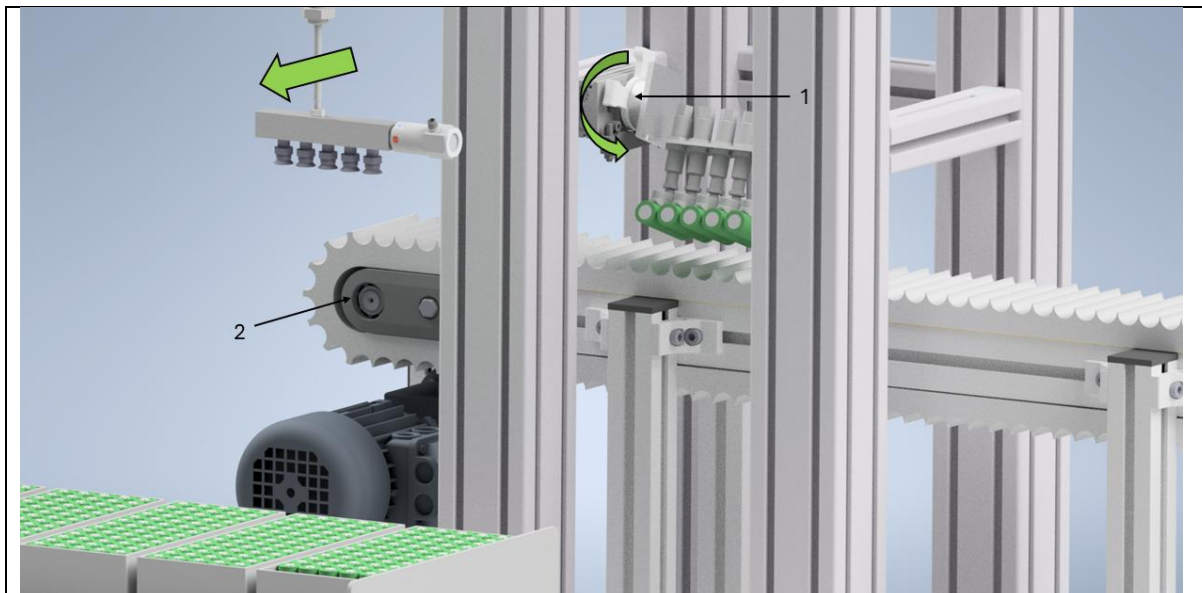


The horizontal electric slider (1), relays the batteries from position A to position B.

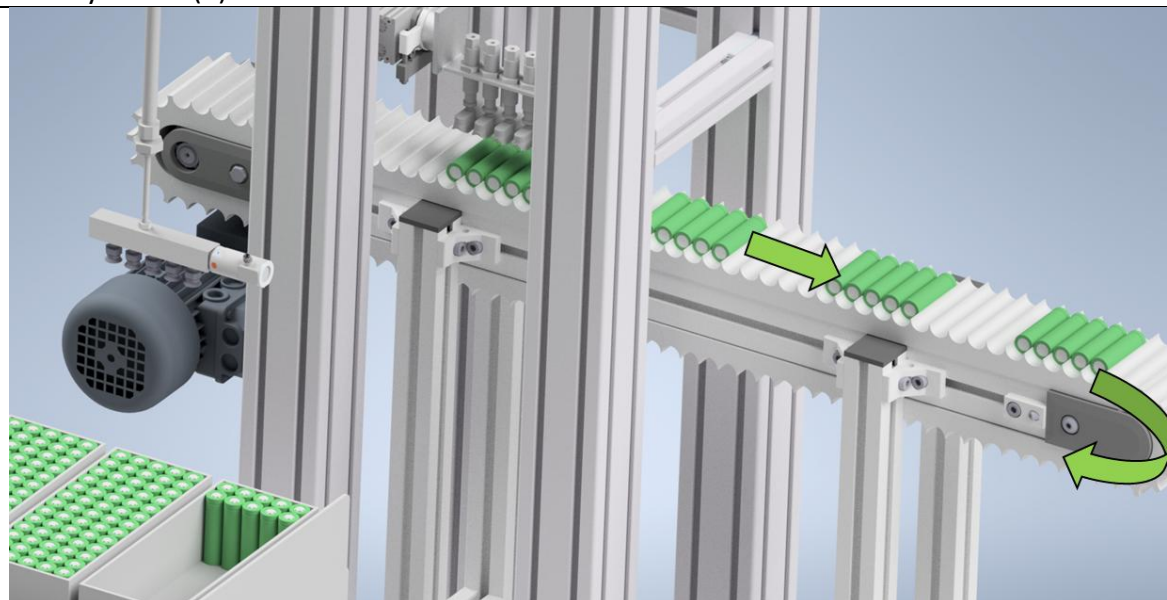


Once the horizontal actuator has contacted the batteries with the concave suction cups (1), pressure valves activate to create a vacuum of 907 Pa for each suction cup. This ensures the batteries are securely held while the solenoid valve (2) deactivates.

Battery Module Assembly

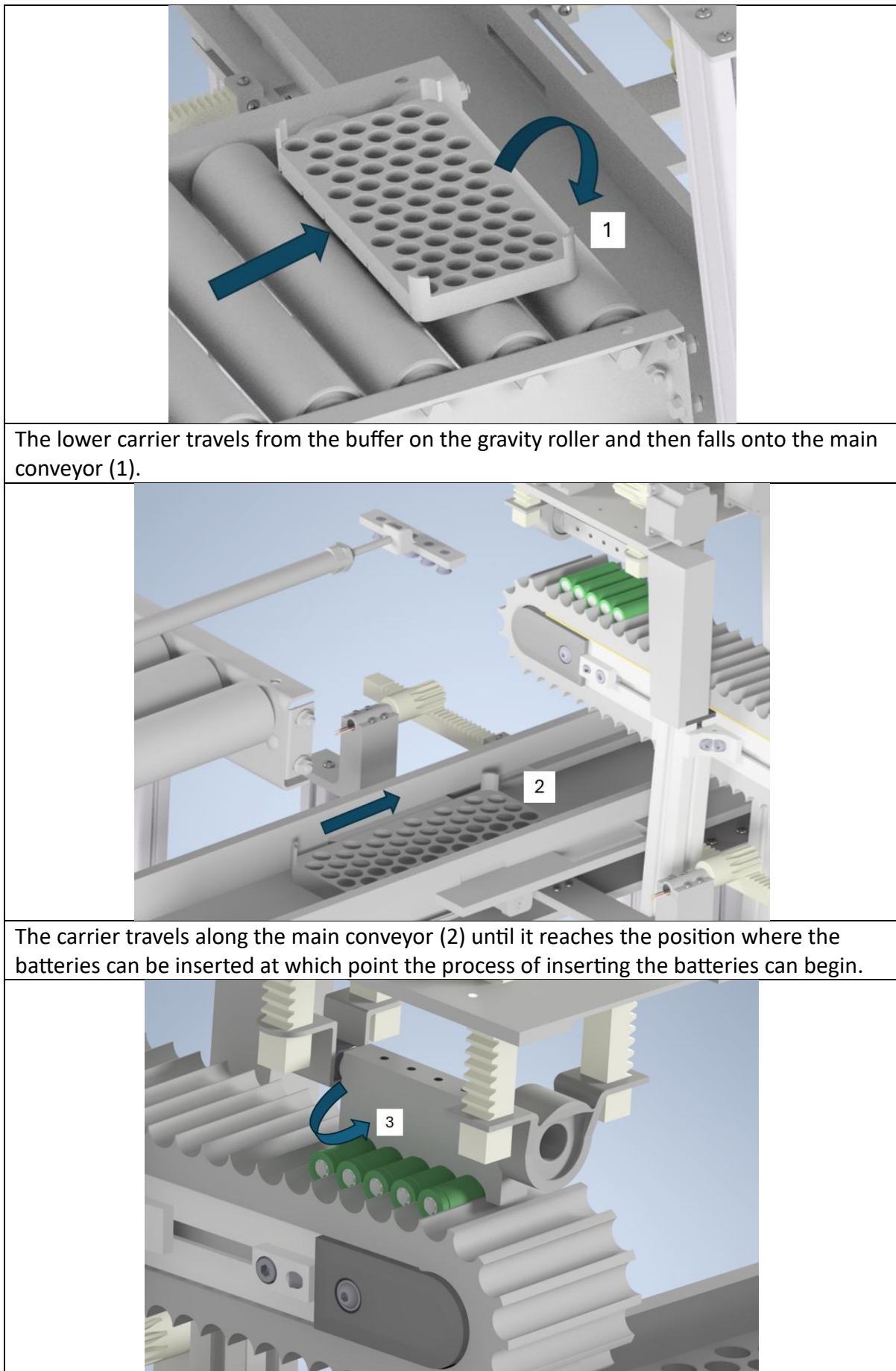


As the horizontal slider returns the vertical actuator to its original position, the rack and pinion pneumatic actuator (1), rotates the 5 batteries by 90 degrees to face the cleated conveyer belt (2).



The conveyor drives without stopping and creates a natural battery buffer of 5 batteries to be collected in the next process of the module assembly.

Battery Module Assembly

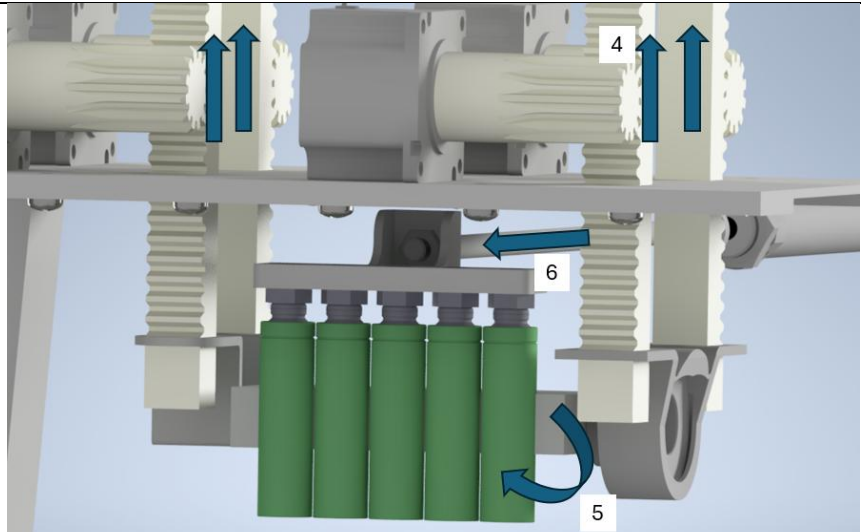


The lower carrier travels from the buffer on the gravity roller and then falls onto the main conveyor (1).

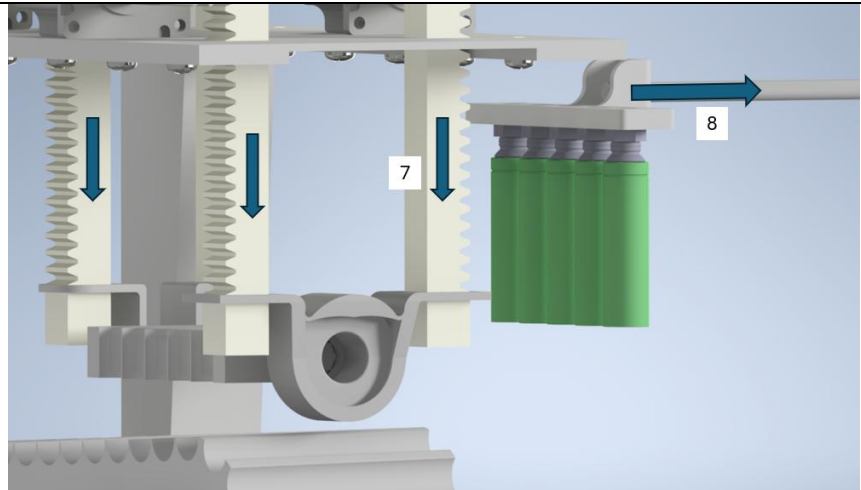
The carrier travels along the main conveyor (2) until it reaches the position where the batteries can be inserted at which point the process of inserting the batteries can begin.

Battery Module Assembly

The suction arm rotates (3) and the solenoid valve creates a vacuum pressure to grab the batteries off of the source conveyor belt.

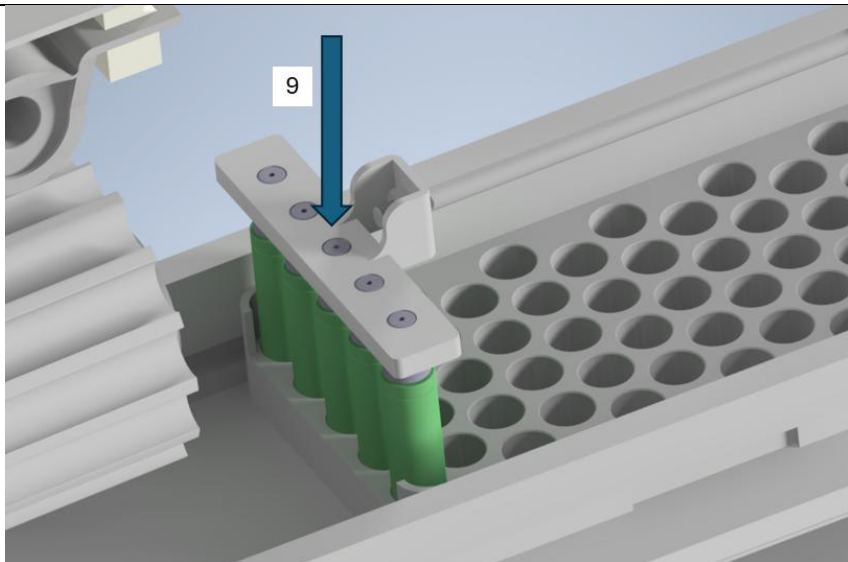


The rack and pinion system activates to move the assembly upwards (4). This gives the batteries enough clearance for the suction arm to rotate to position (5). The horizontal actuator then moves outwards (6) to grab the batteries from the suction arm by activating a vacuum pressure using the solenoid valve. After a pause of 0.5s, the suction arm returns to neutral pressure and the horizontal actuator holds the batteries.

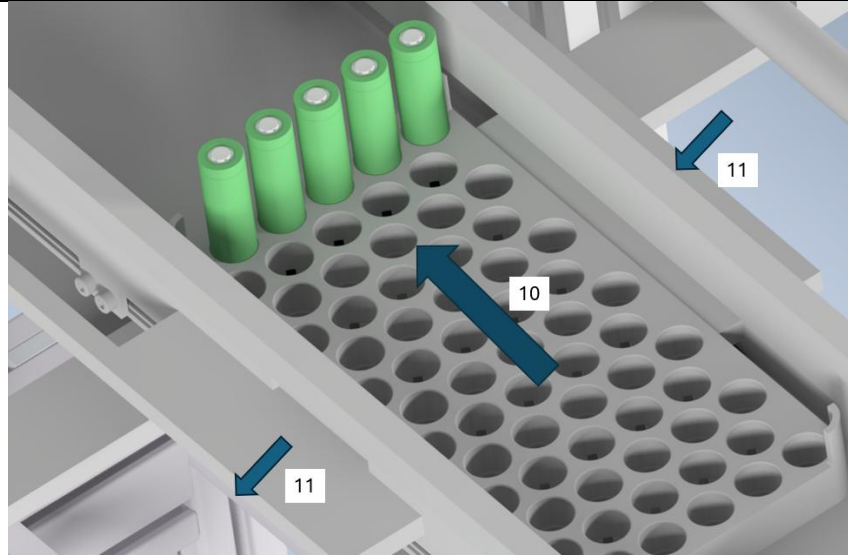


The rack and pinion system then moves downwards (7) to allow for the batteries to be moved away from the assembly by the horizontal actuator. The horizontal actuator moves away from the assembly (7) so the batteries are aligned with the spaces in the lower carrier.

Battery Module Assembly

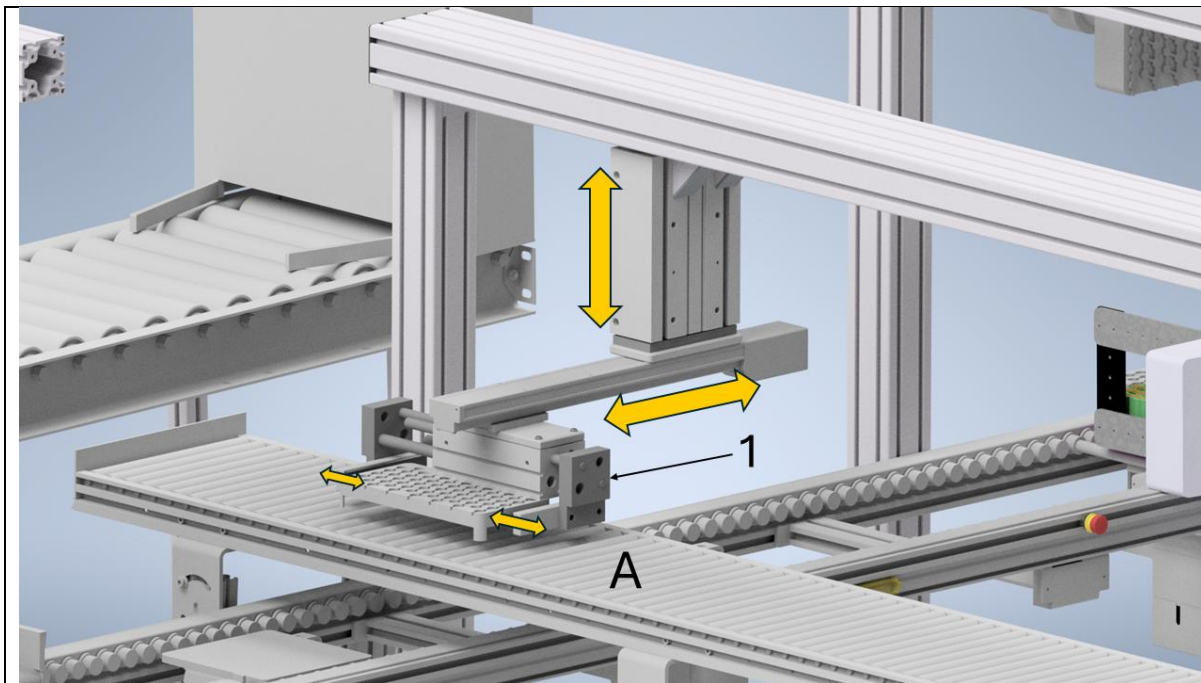


The vertical actuator moves downwards (9) and presses the batteries into the lower carrier with a force of 10N. After this stage, the vacuum pressure creating pressure on the batteries is removed and the vertical actuator returns to its starting position.

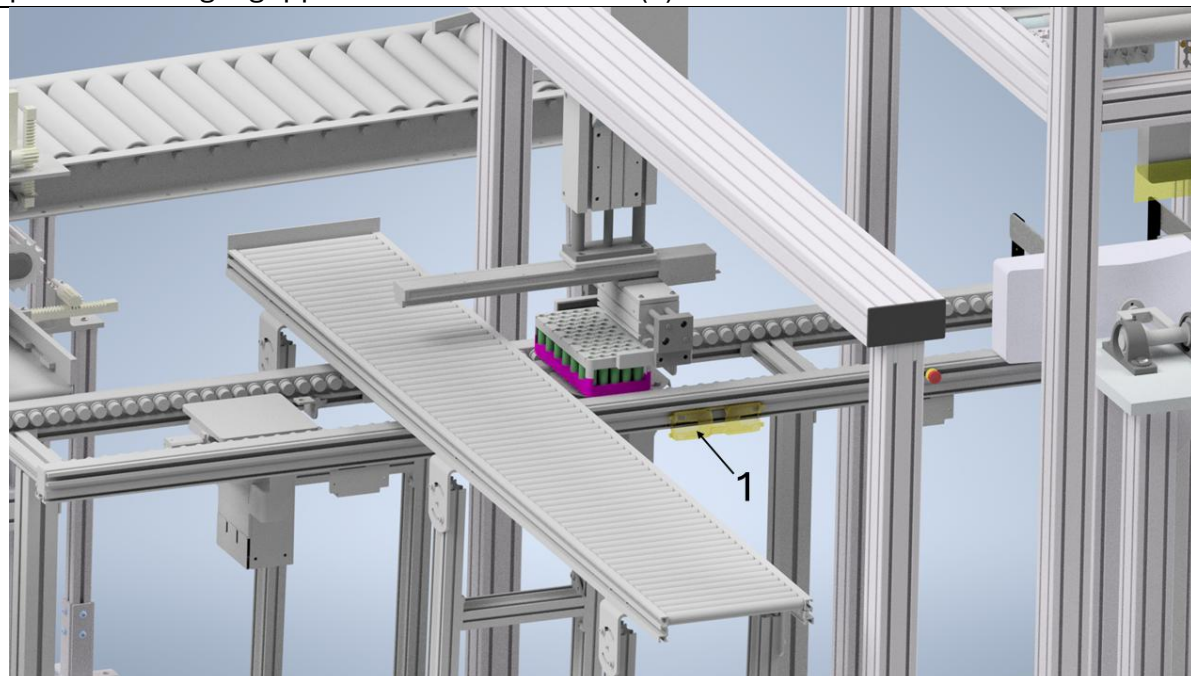


Once the current row of batteries has been placed, the conveyor staggers the carrier forwards (10) so that the next row of batteries can be placed. To ensure the alignment of the holes and cells, the lateral sliders push the carrier by the necessary amount (11).

Battery Module Assembly

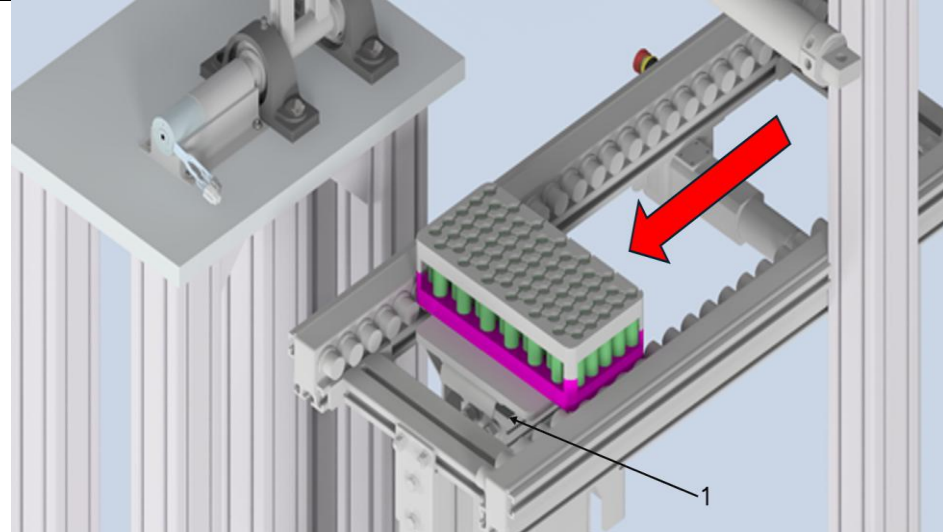


An upper carrier slides down gravity rollers and comes to rest at the bottom of the slope (A). The electric actuator is triggered by an open loop controller and the pneumatic finger grippers close on the carrier (1).

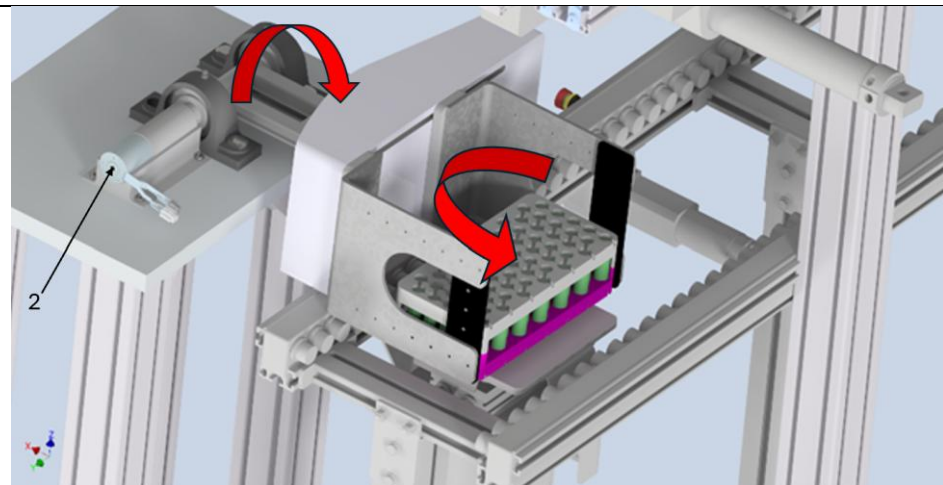


The electric actuator moves back to original position with lower carrier and batteries positioned underneath. A large pneumatic actuator presses upper carrier vertically downwards on top of batteries applying force until the PNP sensor reads 650N of force (1). The actuator then retracts and the cycle resets.

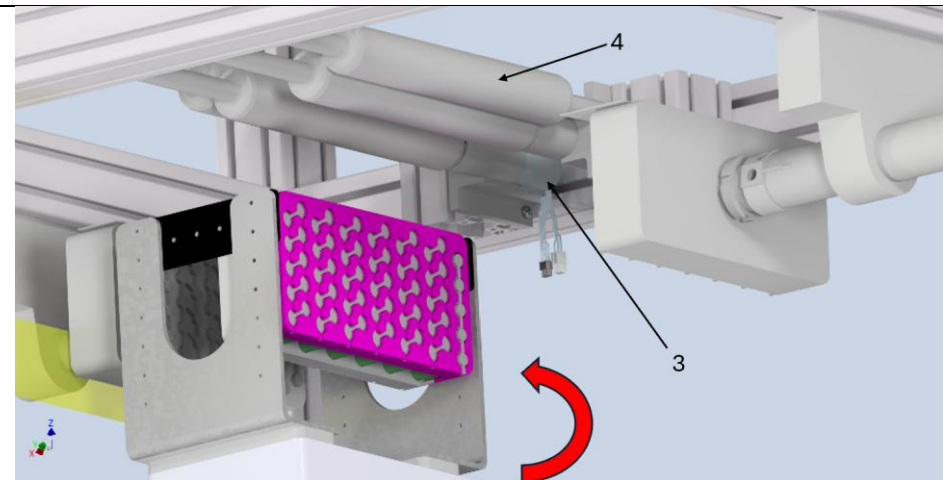
Battery Module Assembly



The module arrives with both carriers and all batteries already placed in previous stages. When the module trips the conveyor stopper (1), the plate lifts up.



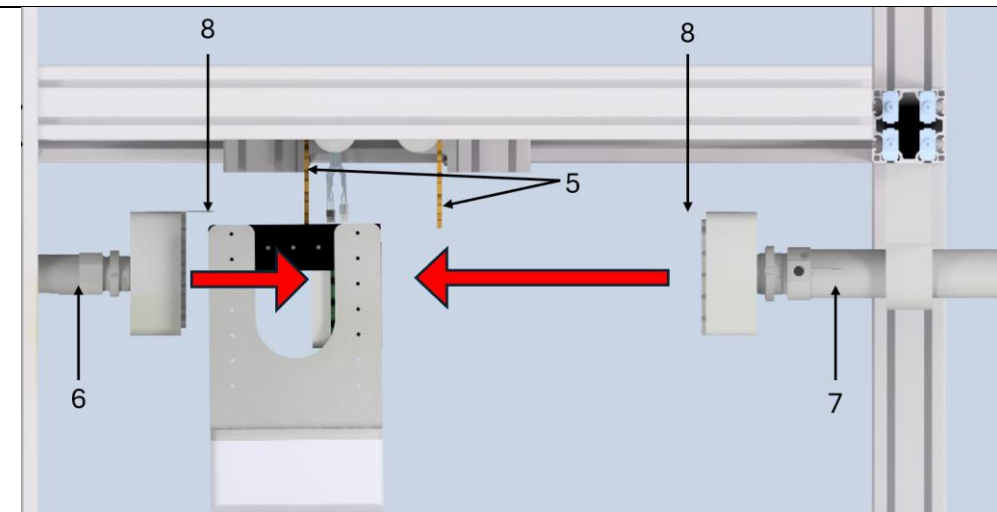
After the conveyor plate has been lifted, the plate is rotated 90 degrees. The arm motor (2) then rotates 90° downwards and the finger grippers clamp the module along the short side.



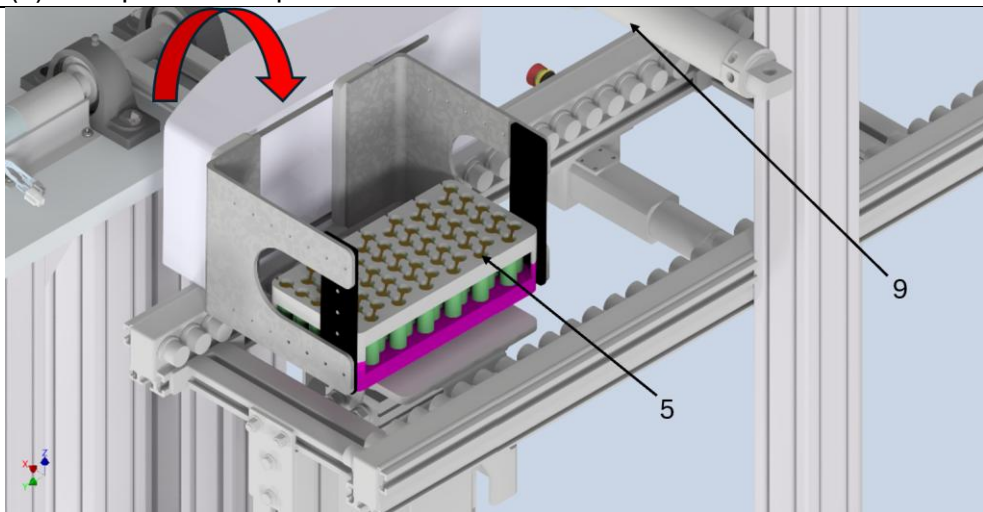
The gripper arm then rotates 90° anticlockwise, lifting the module so that both ends of the batteries are exposed. A sensor on the tape roller motors (3) is triggered. This

Battery Module Assembly

causes the rollers (4) to undergo a set number of revolutions until there is enough tape.



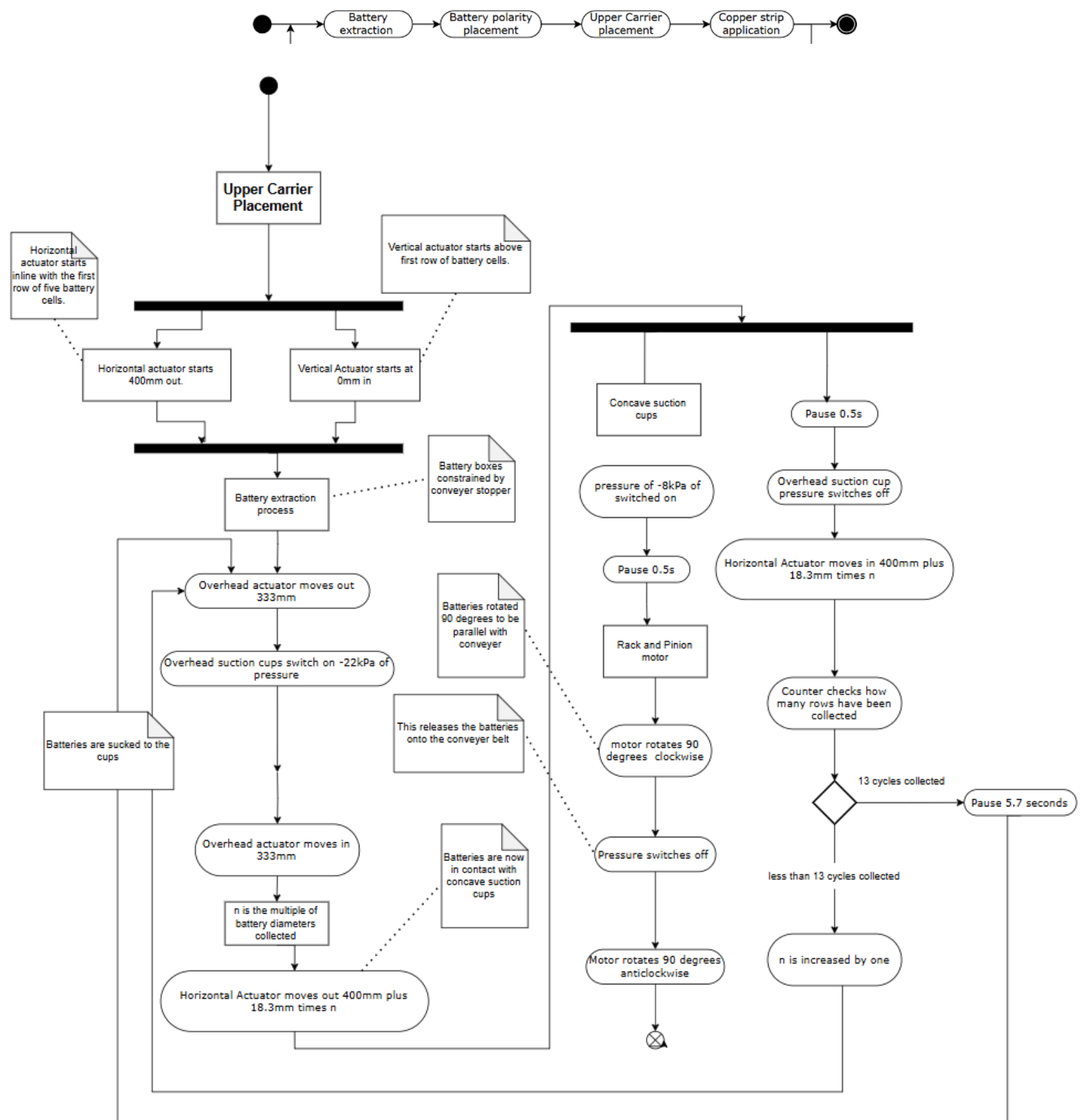
Once the strips (5) have lowered a sensor activates both the short (6) and long (7) pneumatic actuators which press tape to both sides simultaneously. The tape roller motors reverse for a short amount of time and this induces tension allowing the blades (8) on top cut the tape.



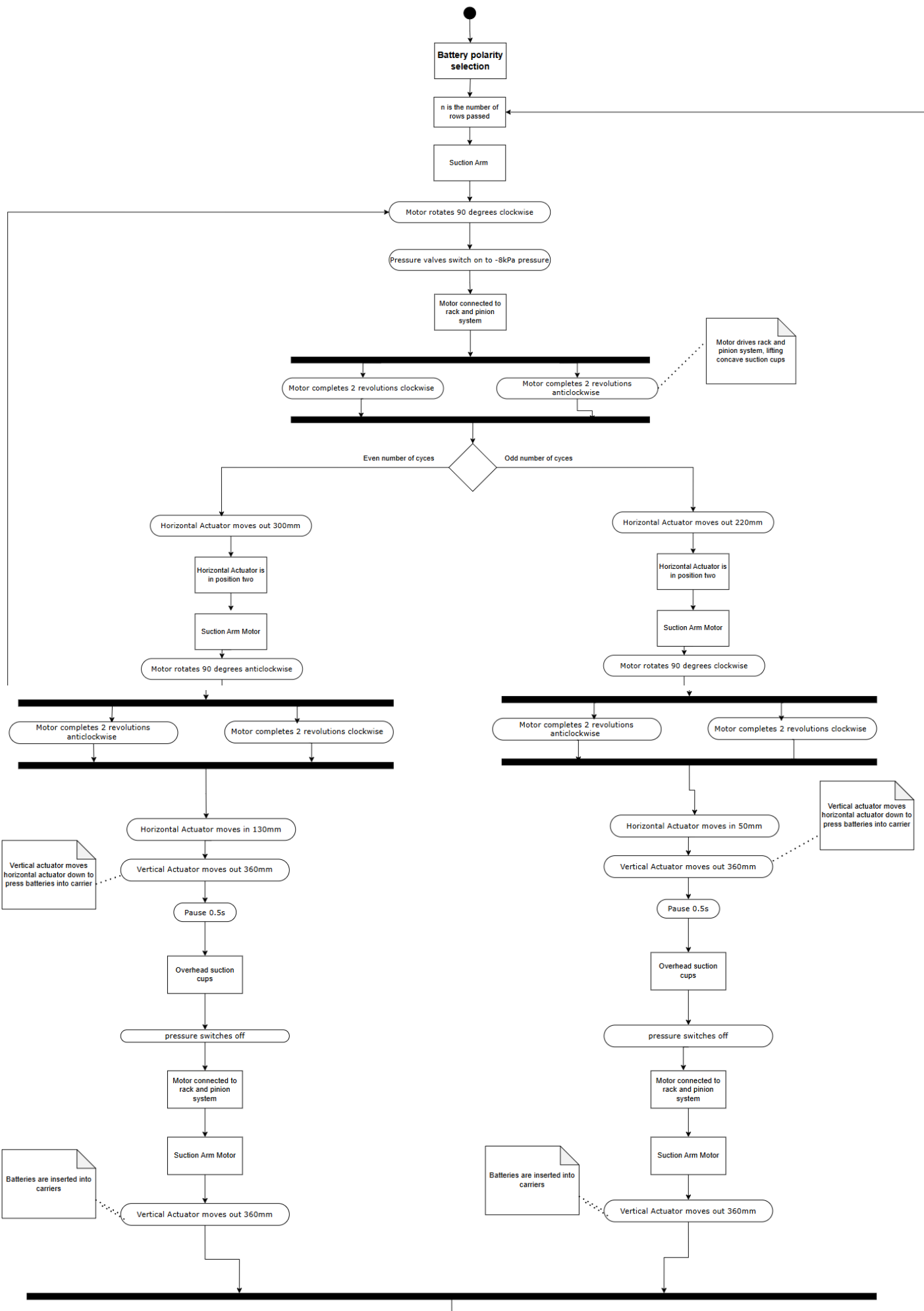
The actuators stop and retract when the D-M9P (9) pressure sensor detects enough force has been applied. Once the actuators retract, the arm returns the module to the conveyor. With the copper strips now applied the module can be ejected from the machine.

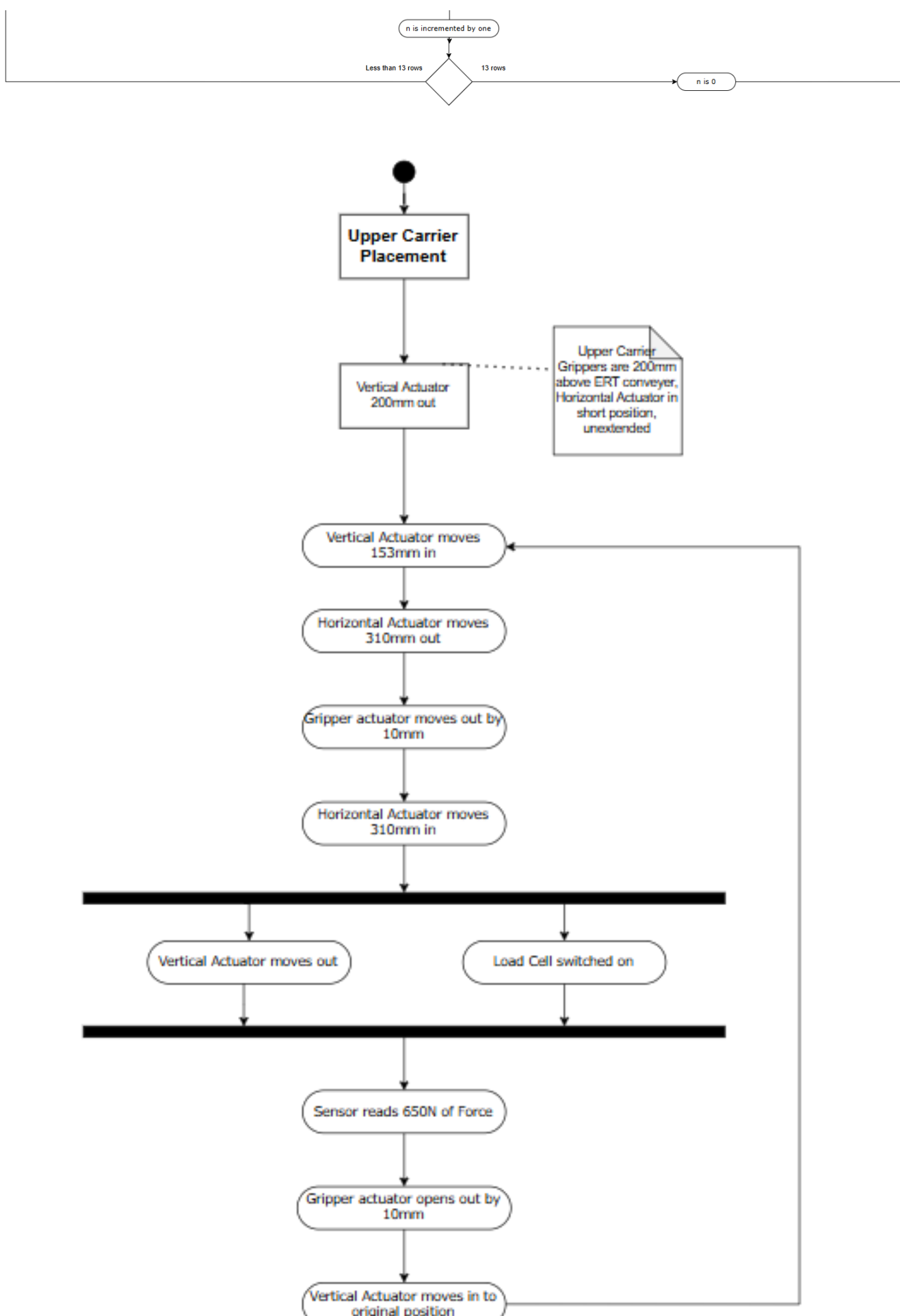
3.7 UML Activity Diagram

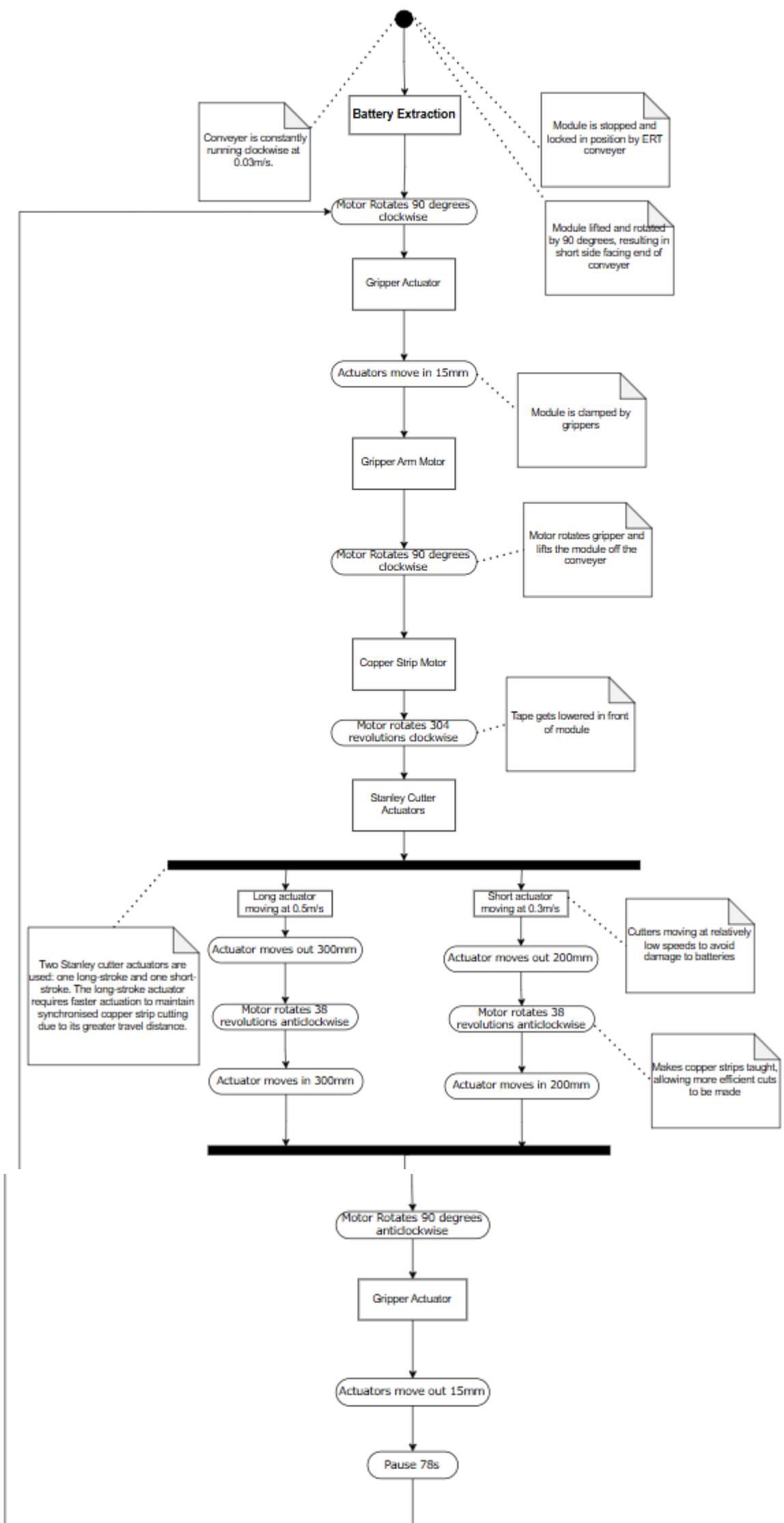
SYSTEM OVERVIEW



Battery Module Assembly







Battery Module Assembly

3.8 FMECA & Fault Tree Analysis

Part name	Function	Potential Failure mode	Cause	Effect	Frequency	Severity	Detection	Risk priority number	Predictive maintenance
Suction cups	Extracts batteries in rows of 5 using pressure suction	Excessive material wear at suction rim	Impact with battery cells during repeated pick-and-place cycles	Loss of suction pressure → Failed pickup → Production delay due to repeated reattempts	3	3	6	54	Inspect suction rims regularly. Replace cups after defined cycle count.
		Filter Blockage	Debris collection in the filter due to lack of maintenance	Vacuum pressure drop → Overheating of pump → Reduced system efficiency	5	1	4	20	Implement regular filter cleaning schedule. Use filter clog indicators.
Pneumatic Actuator	Vertically move suction cups	Actuator sticking during motion	Lack of lubrication between sliding surfaces	Vertical misalignment → Failed pickup or drop-off of batteries	1	4	2	8	Lubricate actuator guide rails regularly. Add lubrication check to maintenance checklist.
		Binding of actuator shaft	Debris inside actuator cylinder	Jittery or uneven motion → Misplacement of suction head	1	4	2	8	Install fine mesh filters before actuator. Clean actuator internals during shutdown maintenance.
		Internal piston damage	Debris inside actuator chamber	Reduced stroke length → Incomplete suction cycle	1	6	5	30	Inspect piston seal integrity during service intervals. Use filtered compressed air.
		Air leakage in actuator	Poor sealing or worn O-rings	Unstable motion → Inconsistent positioning accuracy	2	2	7	28	Replace O-rings periodically. Perform air-leak tests weekly.
Electric slider	Horizontally move suction cups	Actuator deflection	Consistent offset in centre of mass	Tilted motion → Suction cup misalignment with battery rows	1	8	6	48	Balance load distribution on slider. Use stiffer actuator rail if needed.
		Transmission gear wear	Continuous vibrations in gearbox	Loose connections → Imprecise positioning	2	6	9	108	Monitor vibration levels. Use hardened gear material or damping elements.
		Slider jamming	Debris build-up in guide rails	Slider gets stuck → Entire pickup system halts	3	2	2	12	Clean guide rails weekly. Add brush wipers to prevent debris ingress.
		Loss of power to motor controller	Disruption in power supply	System shuts down → Battery transfer fails	1	8	1	8	Check power supply wiring and connectors. Add UPS backup if critical.
		Slider deformation over time	Continuous impact with mechanical stoppers	Misalignment of suction cups → Battery row inconsistency	1	5	7	35	Limit travel stop impact with rubber dampers. Use fatigue-resistant slider materials.
Concave suction cups	Relays batteries from the suction cups to the conveyor	Material wear at contact surface	Repeated impact with battery cells	Degraded suction → Failed battery relay → Production disruption	3	3	6	54	Replace suction cups after wear threshold. Monitor wear visually or via force feedback.
		Filter clogging	Particles collecting in filter	Vacuum inefficiency → Overheating of secondary pump	5	2	4	40	Add filter maintenance alerts. Clean or replace filter monthly.
		Batteries slippage during handover	Insufficient friction between cup and battery	Dropped or misaligned batteries → Retry needed	2	6	1	12	Apply anti-slip coating or use cups with improved grip texture.
		Overloading of suction cups	Vacuum pump not calibrated for battery weight	Multiple batteries dropped → Production retries triggered	1	3	1	3	Verify vacuum pressure against battery weight. Adjust pump settings accordingly.
Rack and Pinion Powered motor	Rotates concave suction cups 90 degrees	Gear tooth wear	Long-term corrosion	Reduced torque transmission → Slower or incomplete rotation	1	3	8	24	Lubricate and inspect gear teeth regularly. Use corrosion-resistant materials.
		Gear jamming due to interference	Poor meshing from worn teeth	Motor stalls → Possible part damage or misalignment	1	4	5	20	Ensure proper gear alignment. Replace worn gears at early signs of damage.
		Motor casing deformation	Excessive contact with external stoppers	Alignment loss → Suction head rotates inaccurately	1	4	7	28	Reinforce motor casing. Use shock absorbers to prevent deformation from impacts.
Conveyer belt	Buffers batteries in place holders	Motor jamming	Debris entering motor housing or drive system	Motor burn-out → Conveyor halt → System backlog	2	5	1	10	Install cover over motor. Clean housing and check alignment weekly.
		Belt slippage due to wear	Belt coefficient of friction degrading from wear/Drivetrain too fast	Delayed handoff → Batteries jam in buffer zone	3	2	4	24	Monitor belt friction coefficient. Replace belt when slip threshold is reached.
		Batteries misalignment with cleats	Rack and pinion not being in phase with conveyer belt	Batteries out of alignment → Not arranged in rows	3	4	2	24	Synchronise rack and pinion with conveyor logic. Calibrate timing using sensor feedback.

Table 8 is the FMECA table that determines the risk priority number of failure modes for components within the first subassembly. Frequency, severity and detection are ranked out of 10.

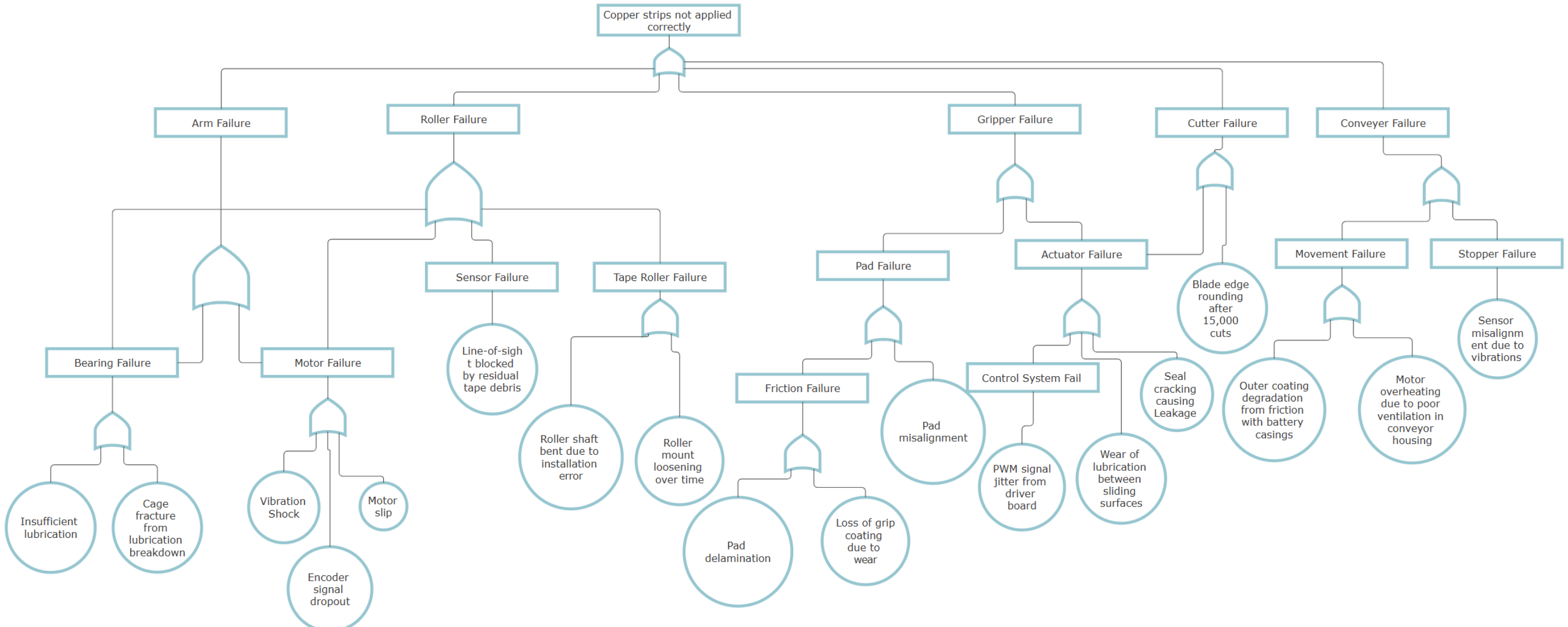


Figure 18 shows the FTA for the fourth subassembly of the machine.

3.9 Solution Specification

Features		Dimensions				
<ul style="list-style-type: none"> <i>Use for product:</i> Battery Module Manufacture <i>Cycle time:</i> 107.68 seconds <i>Cost:</i> <i>Required air pressure supply:</i> 6 bar <i>Power supply:</i> UK single-phase (220 V) <i>DC Components present so rectifiers needed</i> <i>£ 19,900</i> 		<ul style="list-style-type: none"> <i>Overall:</i> 3.301 x 3.206 x 2.29m <i>Conveyor Height:</i> 1m 				

Table 9 Details the features and key dimensions of the machine for its solution specification.

MD_61 Sub Assemblies	Sub Assembly 1	Part Number	Quantity	Part Name	Supplier	Description	Price (£)	Total cost (£)	Sub Assmebly Cost (£)	Duration of operation (s)		
		1.01	5	PFYN 15 NBR-55 G1/8-AG	Schmalz	Suction cups for batteries	3.97	19.85	4023	5		
		1.02	5	SOG 15x40 N - M5M	AirBest	Concave suction cups for batteries	8.43	42.15				
		1.03	1	EQFS 25 LHH-700-B6	SMC	Electric slider for horizontal battery extraction	930	930				
		1.07	1	25A-C85Y12-36	SMC	Pneumatic actuator for vertical battery extraction	120	120				
		1.08	1	DRRS-12-180-FH-PA	Festo	Pneumatic rack and pinion motor for battery rotation	531	531				
		1.09	5	PSPT -110 G1F - M16	AirBest	Level compensators for concave suction cups	32	160				
		1.10	6	UVVG-S10	Schmalz	Solenoid valves for accurate pressure distribution	17	102				
		1.11	1	Connecting L plate	Custom	Connection between rotary actuator and batteries	23	23				
		1.12	1	Actuator Casing	Custom	Electric slider actuator housing						
		1.13	1	Valve Connector	Custom	Connection plate between valves and pneumatic actuator						
		1.14	1	Cleated PVC Belt	Custom	Cleated belt to buffer batteries in place	20	20				
		1.15	1	GUF-P 2000 AG/1000/100	mk Technology Group	Battery buffer conveyor	1140	1140				
		1.16	1	Frame 1	item24	Support frame for the entirety of Sub Assembly 1	935	935				
	Sub Assembly 2	2.01	4	Pinion Motor	Maxon	Rotates the pinion gear to raise the racks	119.98	479.92				
		2.02	4	Rack	RSComponents	To raise the suction subassembly	39.88	159.52				
		2.03	1	Motor Housing	Custom	Rotates the suction arm	3.1	3.1				
		2.04	5	SOG 15x40 N - M5M	AirBest	Concave suction cups for batteries	8.43	42.15				
		2.05	1	Bearing Housing	Simply Bearings	Houses the bearing for rotating the suction arm	30.73	30.73				
		2.06	1	Base Plate	Custom	Plate for components to be mounted on	10.11	10.11				
		2.07	4	Pinion Gear	RSComponents	Pinion Gear to lift the rack	8.83	35.32				
		2.08	1	Rotation Motor	Maxon	Motor to rotate the suction arm	96.35	96.35				
		2.09	1	End Cap of Suction	Custom	Acts as the end cap for the suction arm subassembly	10.01	10.01				
		2.10	1	Bearing Connection	Custom	Connects the bearing to the suction arm subassembly	5.06	5.06				
		2.11	1	Bearing	RSComponents	Allows the suction arm subassembly to rotate	4.31	4.31				
		2.12	1	Horizontal Actuator	SMC	Moves outwards to grab batteries from suction arm	314.11	314.11				
		2.13	1	Main Rear Support	item24	Supports the entire subassembly	164.44	164.44				
		2.14	1	Vertical Actuator	Tolomatic	Moves the batteries downwards to be inserted	699	699				
		2.15	1	Top of Rear Support	Custom	Joins onto the top of the rear support	5.32	5.32				
		2.16	2	Floor Support	item24	Joins the rear support onto the floor	15.6	31.2				
		2.17	1	Actuator Housing	Custom	Joins the horizontal actuator onto the vertical one	35.18	35.18				
		2.18	1	Lower Actuator Support	Custom	Provides a support for the lower actuator	5.16	5.16				
		2.19	1	Suction Cup Housing	Custom	Provides a housing for the suction cups	40.2	40.2				
		2.20	5	PFYN 15 NBR-55 G1/8-AG	Schmalz	Suction cups for batteries	3.97	19.85				
		2.21	1	Main Conveyor	item24	Main assembly conveyor belt	1423	1423				
		2.22	2	Motor Support	Custom	Provides a support for the motor	19.86	39.72				
		2.23	8	Support Frame Feet	item24	Allows the motor supports to be joined to the floor	15.9	127.2				
		2.24	4	Main Frame	item24	Provides the main suppor for the conveyor	21.3	85.2				
		2.25	1	Conveyor Underside	Custom	Allows the conveyor to be joined to the supports	28.66	28.66				
		2.26	2	Carrier Pushers	Custom	Moves the carriers laterally to align the battery holes	5.21	10.42				
		2.27	2	Horizontal Racks	RSComponents	To raise the suction subassembly	39.88	79.76				
		2.28	2	Motor Supports	Custom	Provides a secure motor base	5.24	10.48				
		2.29	2	Motor Lower Housing	Custom	Lower housing for the motor	5.02	10.04				
		2.30	2	Pinion Motor	Maxon	Rotates the pinion gear to raise the racks	119.98	239.96				
		2.31	2	Motor Upper Housing	Custom	Upper housing for the motor	5	10				
		2.32	2	Pinion Gear	RSComponents	Pinion Gear to lift the rack	8.83	17.66				
		2.33	1	Gravity Roller	Dorner	A gravity roller to provide the lower carrier	1000	1000				
		2.34	2	Connection to Conveyor	Custom	Connects the suction subassembly to the battery conveyor	20.32	40.64				
		2.35	1	Main Base Platform	Custom	Raises the entire subassembly	68.75	68.75				
		2.36	2	Smaller Struts	Custom	Raises some legs of the subassembly	13.14	26.28				
	Sub Assembly 3	3.01	1	MGPM63TF-200Z	SMC	Compact guide cylinder	552	552	2514.5	5.61		
		3.02	1	LEFS25GA-400N-R3C6H83	SMC	Electric slider type, ball screw	832.5	832.5				
		3.04	1	MHL32-32D2	SMC	2 finger gripper	450	450				
		3.05	1	Grippers	Custom	Custom grippers	25	25				
		3.06	1	Adaptor	Custom	Custom adaptor	25	25				
		3.07	1	Frame 2	item24	Support frame for top carrier application	630	630				
		4.01	1	2FGP20	OnRobot	Module gripper	£1,000	£1,000				
		4.02	2	Pads	OnRobot	Gripper pads	£5	£10				
		4.03	1	ISO Flange	Kempi	Flange for connecting arm to gripper	£10	£180				
		4.04	6	HPC 30mm Pillow Block	HPC	Bearings for various shafts						
		4.08	1	Gripper Arm	Custom	Gripper Arm	£1.17	£1.17				
		4.09	3	EC-i40, 100 Watt	Maxon	Motors for all copper strip functions	£838.84	£838.84				
		4.10	1	GPX 42 UP Ø42 mm	Maxon	Gearhead for arm motor	£568.87	£568.87				
		4.11	10	Bolt	item24	Bolts	£5	£5				
		4.13	8	ISO M4 Screw	item24	Screw	£7.60	£7.60				
		4.14	10	BS Nut + Washer	item24	Nut+Washer	£6.35	£6.35				
		4.16	4	Copper tape roller	Custom	Rolls out copper strips for application	£491.36	£491.36				
		4.17	4	Copper tape roller holder	Custom	Holds ends of the rollers	£14	£14				
		4.19	2	Tape Cutting Angled Blade	Custom	Cuts tape after application	£265.50	£265.50				

3.10 Manufacturing Operations

Plant Layout

The goal of the plant layout is to minimise the wasted time that occurs when transporting materials from one location to the other. The first stage of determining an effective plant layout was to compartmentalise the resources of the plant into the departments shown below.

Department Number	Department Name
1	Storage area for all hoverboard components
2	Technician's area
3	Administration offices
4	Equipment cabinet
5	Autonomous Mobile Robot (AMR) room
6	Entry
7	Exit
8	Battery module assembly area
9	Completed hoverboard storage
10	Accumulator and hoverboard assembly
11	Quality Assurance (QA) area

Table 11 compartmentalises different departments within the plant.

To minimise the tasks of the technicians and increase the efficiency of the plant, Autonomous Mobile Robots (AMR) made by SMC were utilised. Their roles include the transportation of raw/waste materials and finished products to the necessary areas. The AMR room would contain docking stations for these robots alongside any equipment needed for their maintenance. The equipment cabinet would contain more general equipment for other sections of the plant. Once the departments were chosen, the relationships between the departments were decided based off positive and negative interactions that could arise through the arrangement of departments and were then arranged into an overall relationship matrix.

Code	Desired Relationships	Value
A	Absolutely Necessary	4
E	Especially Important	3
I	Important	2
O	Ordinary	1
U	Unimportant	0
X	Undesirable	-1

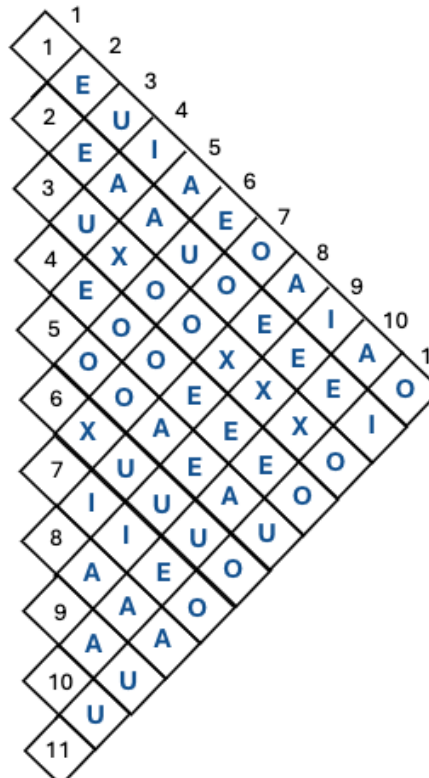
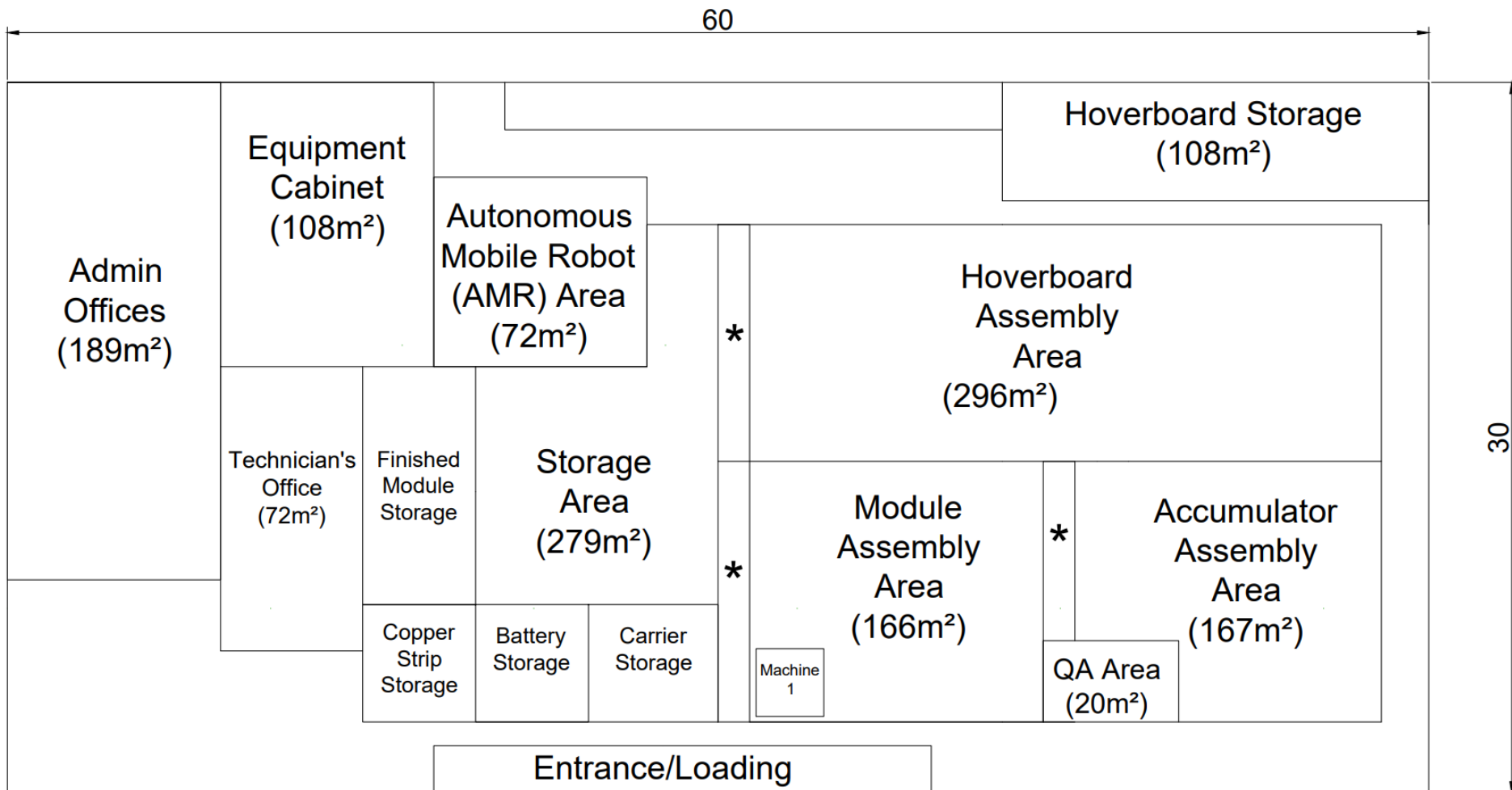


Table 12 evaluates the relationship between each department within the plant. It decides, why certain departments should be closer to each other compared to others.

This relationship matrix was then used to create and refine a relationship diagram which was then used to create a floor plan for the plant as shown on the next page.

Battery Module Assembly



* – Short term storage for the local assembly area

Machine 1 – The machine described above in the report

Figure 19 displays the plant layout on a floor plan.

Battery Module Assembly

The overall plant follows a product layout where the resources are grouped according to the sequence of operations required by the parts. This layout is the most efficient for the high-volume production expected of the plant as it allows for the efficient movement of products from one assembly stage to the next.

The plant layout design was created using some assumptions. Primarily, it was assumed that no critical support pillars would obstruct department placement, and that power sockets and pressure sources were evenly distributed throughout the facility. Additionally, it was assumed that there were no predetermined constraints on department locations.

The administration offices were positioned away from the assembly areas to minimize noise disruptions. The storage area was placed near the assembly zones to reduce material handling times. To greater optimize efficiency, the AMR room was positioned adjacent to storage and assembly areas, further reducing material transport time. The hoverboard assembly area was designed larger than other sections to accommodate the final product's size. A short-term storage area would provide a local buffer of raw materials, easing the material handling workload on technicians. The entrance was centrally located for convenient worker access and to minimize restocking time for raw materials. Similarly, the exit was placed next to hoverboard storage to expedite the export of finished products.

Material Flow

Due to the plant layout having the material handling areas (unloading, storage, assembly and export) close together, the material handling time for the process is minimised. Since the time longest step of the process takes 78.2s , the rate of consumption of raw materials will use this value. The intervals at which each resource would need to be replenished depend on the buffer size and the time taken to transport the material from storage to the assembly area. The AMRs in charge of transporting the materials operate a speed of 1ms^{-1} . The intervals between the restocking of each raw material is shown in the table below.

Raw Material	Buffer Size	Gross time between restocks (mins)	Distance to storage (m)	Time spent in transit (mins)	Net time between restocks (mins)
Lower/Upper carriers	30 carriers	39	1.5	0.025	38.98
Boxes of batteries	50 boxes	65	7	0.117	64.88
Copper rolls	100 metres	1000	11.5	0.192	999.81
Finished modules	60	78	13.5	0.225	77.78

Table 13 defines the material flow through the plant.

The much longer restock time for the copper rolls justifies its placement furthest away from the machine as the longer transit time will have a negligible impact on the net time between restocks. Conversely, since the carriers have the fastest restock time, they were placed the closest to the machine.

Resource route	Distance to travel (m)
Raw resources from entrance to storage	8
Hoverboard assembly to hoverboard storage	3
Finished hoverboards from storage to export	5

Table 14 shows the distances between resource routes.

The placement of the hoverboard storage between the export and the assembly area is justified by the short distances between the departments (as seen in table above) which reduces the required material handling time. The short distance between the entrance and the main storage area also reduces this time.

Capacity and Inventory

There are various considerations and timespans for a 20% increase in battery module demand. The strategy outlined here treats the 20% increase as a medium-term seasonal increase which would coincide with summer demand for hovercraft when there is less rain, but also general demand increases when the product gains popularity. The long-term assumption is that demand increase would continue for multiple years.

There is a large 279m² storage area which will hold all inventory. There are various types of inventory present in this operation and some intermediate stages which cannot be stored. The initial raw parts inventory which can be stored easily includes the battery boxes, the upper and lower carriers and the copper strips. It takes much longer to produce all the modules for the accumulator than making the accumulators themselves and this limits production speed. The completed module however can be stored until demand increases and accumulators need to be put together and placed into hovercraft.

The general inventory ordered in throughout the year will feature an amount of buffer in case the demand increases faster than expected. Enough carriers, batteries and copper will be supplied with every order so there will never be too few of either to make a module. The number of completed modules the machine will produce will be increased as demand increases. The initial rate of module production will be 1106 modules a day. The machine running at full speed however can achieve 1660 a day although at increased power costs so timing this with the demand is key. This 34% maximum potential increase exceeds requirements.

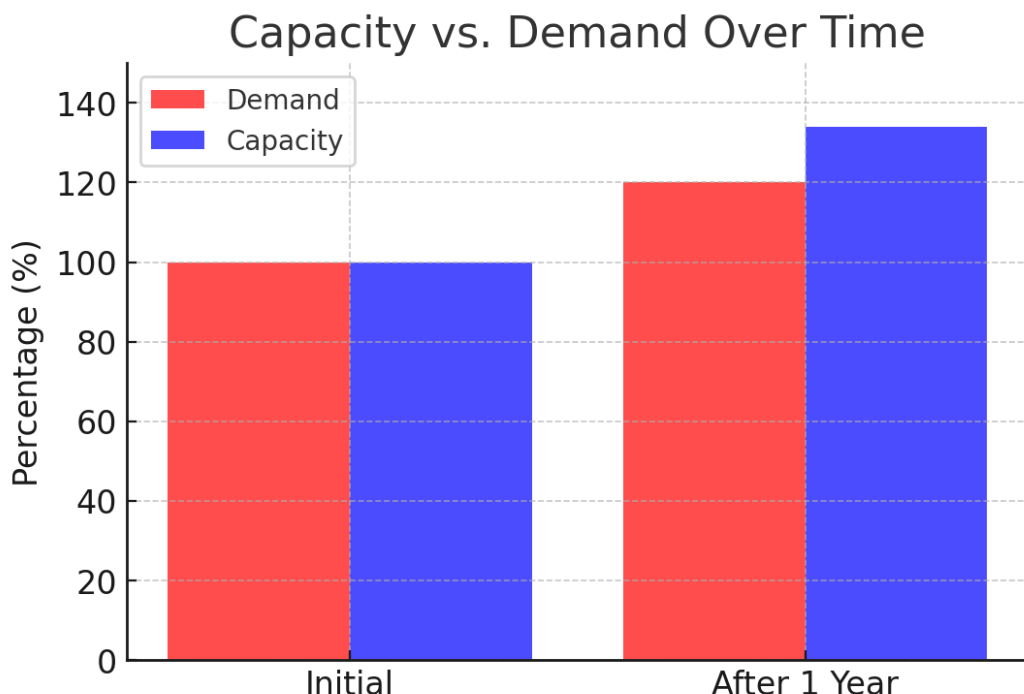


Figure 20 shows the capacity vs demand over time.

Battery Module Assembly

Initially when demand is low completed modules can be held as anticipation inventory ready to be used in the hovercraft when demand increases. There are risks associated with storing batteries including leaks and internal short circuits and so tightly packing modules is not feasible. Because it is safer to store fewer modules, the minimum amount of anticipation possible will be kept in storage. When demand does increase the anticipation will be ready to be used alongside the modules still coming off the production line reducing the need for drastic production speed increases. In the longer term there is still 14% capacity to be utilised by the machine. There is also a large amount of unused space in the plant due to the compact machine design so new units could be built in anticipation of further demand growth.

Quality Management Plan

First, quality characteristics and the test methods were selected.

The chosen characteristics were structural response to vibration and conductivity during vibration. Looking ahead to the final product, it was assumed that there would be a level of vibration associated with the motion of the hovercraft. It is extremely important that the modules within each accumulator have no broken connections or loose and/or cracked cells as this would be a massive safety and health hazard. Acceptance sampling was chosen as the control method.

Crucial steps occur even during the final stage of the manufacturing process and so quality management was to take place after module completion. It was decided that the test batch of modules would be placed on a vibrating work surface while simultaneously a DC voltage and current multi-meter would test the desired electrical output.

Certain standards were set. With an appropriate level of vibration set to the work surface, a voltage reading would be taken with a deviation of $\pm 3\%$ being acceptable. Structural response would be carried out simultaneously. If batteries were to come loose or carriers slide out of position that would also be considered a failure.

The acceptance sampling rate would be 30 in a test batch. If 5 or more modules fail the voltage test by a small margin, then the batch is discarded and machine operation paused until investigation into cause complete. However, for more serious failures or evidence of dangerous damage, 1 is enough due to the high-risk nature of the product. The plant operates on 3, 8-hour shifts and one test would be carried out per shift.

When a faulty module is found the system would be notified and the module would have to be ejected into a specific space for further inspection. There are numerous possible reasons for a module failing both the electrical and structural tests with copper strip misalignment, loose batteries, cracked batteries and loose carriers being the most likely. Continual improvements and adjustments could be made to the quality control strategy

Battery Module Assembly

as time goes on and sources of defects are identified and understood better. Additionally, the machine could be reworked and tuned to prevent repeated faults.